Heliyon 9 (2023) e16601

Contents lists available at ScienceDirect

Heliyon

journal homepage: www.cell.com/heliyon

Review article

Review on magnetic spinel ferrite (MFe_2O_4) nanoparticles: From synthesis to application

Shameran Jamal Salih [a,b,*], Wali M. Mahmood [a]

[a] Department of Chemistry, Koya University Koya KOY45, Kurdistan Region – F.R, Iraq
[b] Department of Pharmaceutical Basic Sciences, Faculty of Pharmacy, Tishk International University, KRG, Erbil, Iraq

ARTICLE INFO

Keywords:
Spinel ferrites
Magnetic properties
Dopants

ABSTRACT

Magnetic spinel ferrite materials offer various applications in biomedical, water treatment, and industrial electronic devices, which has sparked a lot of attention. This review focuses on the synthesis, characterization, and applications of spinel ferrites in a variety of fields, particularly spinel ferrites with doping. Spinel ferrites nanoparticles doped with the elements have remarkable electrical and magnetic properties, allowing them to be used in a wide range of applications such as magnetic fields, microwave absorbers, and biomedicine. Furthermore, the physical properties of spinel ferrites can be modified by substituting metallic atoms, resulting in improved performance. The most recent and noteworthy applications of magnetic ferrite nanoparticles are reviewed and discussed in this review. This review goes over the synthesis, doping and applications of different types of metal ferrite nanoparticles, as well as views on how to choose the appropriate magnetic ferrites based on the intended application.

1. Introduction

Spinel ferrite materials are metal oxides with spinel structures that have the general chemical formula AB_2O_4, where A and B represent various metal cations that are located at tetrahedral (A site) and octahedral (B site) positions, respectively. The types, quantities, and placements of the metal cations in the crystalline structure have a significant impact on the physicochemical properties of ferrites [1,2].

Due to their unique and remarkable properties, nanocrystalline magnetic materials have attracted attention from various fields, such as physics, chemistry, biology, medicine, materials science, and engineering. Nanomaterials have particle size up to 100 nm and high surface-to-volume ratio, which altered or enhanced reactivity, thermal, mechanical, optical, electrical, and magnetic properties as compared to their bulk counterparts [3–6]. While the chemical composition of bulk materials is the main determinant of their qualities, the particle size, and morphology of nanomaterials, in addition to the chemical composition, dictate the majority of their features. Furthermore, depending on the particle size and chemical composition, these qualities can be fine-tuned [3,7–9]. Ferrites are significant and fascinating materials from both a practical and theoretical standpoint. Magnetic $CoFe_2O_4$, $MnFe_2O_4$, $CuFe_2O_4$, $ZnFe_2O_4$, and $NiFe_2O_4$ nanoparticles have received a great deal of attention owing to their thermal and chemical stability, as well as their distinctive structural, magnetic, optical, electrical, and dielectric properties, and their broad range of technological applications including photocatalysis, photoluminescence, biosensors, humidity-sensors, catalysis, magnetic refrigeration, permanent magnets,

* Corresponding author. Department of Chemistry, Koya University Koya KOY45, Kurdistan Region – F.R, Iraq.
E-mail address: shameran.jamal@koyauniversity.org (S.J. Salih).

https://doi.org/10.1016/j.heliyon.2023.e16601
Received 25 December 2022; Received in revised form 9 May 2023; Accepted 22 May 2023
Available online 26 May 2023

magnetic drug delivery, magnetic (hyperthermia) [10,11].

This work described the thermal, structural, morphological, and magnetic properties of spinel ferrites (MFe_2O_4, M = Cu, Co, Mn, Zn, and Ni) and doped ferrites (Zn^{+2}, Ni^{+2}, Al^{+3}, Mn^{+2}, Ag^{+}, Y^{+3}, Nd^{+3}, Ti^{+4}, Cd^{+2}, Dy^{+3}, Gd^{+3}, Cu^{+2}, Yb^{+3}, Eu^{+3}, Zr^{+4}, In^{+3}, Cr^{+2}, Pr^{+3}, Sm^{+3}, Ho^{+3}, Er^{+3}, Mg^{+2}, La^{+3}, and Ce^{+3}) with different transition metals, produced by Co-precipitation method, Hydrothermal and Solvothermal method, Microemulsion method, High-Temperature Thermal Decomposition method, Sol-gel method, Electrochemical Deposition method, Sonolysis or Sonochemical method, Microwave-Assisted method, and Biosynthesis methods [12–14].

Additionally, the purpose of this paper is to investigate and examine several subjects, including the numerous synthesis methods of MFe_2O_4 and their metal dopants, as well as their benefits and drawbacks, and the most relevant applications in conventional and current technologies.

There are four main sections in the review paper. The classification of magnetic spinel ferrites and a brief overview of ferrites and their structures are all covered in the first section, “Magnetic spinel ferrites”. The second section, “Magnetic properties,” provides a brief overview of magnetic properties in spinel ferrites. The third section, “Synthesis methods,” provides an overview of the main methods in the area of spinel ferrites. The impact of doping on the properties of magnetic spinel ferrites is discussed in the fourth section. The major applications of spinel ferrites are summarized in the final and fifth part, “Applications of spinel ferrites."

1.1. *Magnetic spinel ferrites*

Magnetic spinel ferrite materials have sparked a lot of attention recently because of the vital roles that play in improving scientific knowledge and understanding of magnetic materials in general, and ferrites in particular [15–17]. Ferrites are a class of ferrimagnetic ceramics that are used in a variety of electric and optoelectric devices due to their magnetic properties, high electrical resistance and minimal eddy current losses [18–20]. Spinel ferrites have the typical formula MFe_2O_4, where M is an ion of divalent metal and Fe is in the +3 oxidation state [21]. Ferrites are materials having a wide range of physical qualities, as well as low production costs and great chemical stability. Ferrites differ from garnet, hexagonal, and spinel in structure depending on their initial crystal lattice. There are 64 tetrahedral and 32 octahedral sites in a single unit cell, however, only 8 and 24 sites are filled by cations, respectively [22] (Fig. 1a). Based on the cations distribution in the octahedral and tetrahedral sites, there are three types of normal, inverse, and mixed spinel.

As a result, the typical example for normal spinel (Fig. 1b) is $ZnFe_2O_4$ where the Fe^{3+} ions are found in the octahedral sites while Zn^{2+} ions are located in the tetrahedral sites. In addition, inverse spinel (Fig. 1c) is $NiFe_2O_4$ where Ni^{2+} ions and half of the Fe^{3+} ions are in the octahedral sites and the remaining half of the Fe^{3+} ions are in the tetrahedral sites [23]. This implies that the cation distribution between the two interstitial sites may have an impact on the magnetic properties of spinel ferrites [24–29].

Among spinel ferrites, cobalt ferrite ($CoFe_2O_4$) with high Hc, large cubic magnetocrystalline anisotropy, and moderate saturation magnetization (Ms) is regarded as a hard-magnetic material. Due to these characteristics, it can be used for magnetic storage and a number of other applications [32]. In biomedical applications, it could be utilized for magnetic separation, magnetic resonance imaging, magnetically directed drug delivery, and hyperthermia for cancer treatment. It can be employed in industrial applications as bare nanoparticles for pollutant removal by adsorption or photocatalytic degradation. The essential features of $CoFe_2O_4$ NPs, such as their high Ms value, visible light absorption capacity and low bandgap energy of 2.04 eV have attracted interest [33,34]. Cation distribution, Ms, and chemical and physical characteristics as well as crystallinity and surface area of $CoFe_2O_4$ have all been found to be influenced by synthesis procedures [15,35,36].

$ZnFe_2O_4$ NPs, one of the most important ceramic materials, have attracted attention in many applications due to their distinctive properties including high magnetic permeability, high Curie temperature, high electrical resistivity, low power loss [37,38]. Due to their exceptional features, magnetic spinel material can be used for numerous technical applications, such as transformer cores, read/write heads for high-speed digital cassettes, radio frequency circuits, and absorbers for electromagnetic waves. It’s also a great addition to biomedical diagnostic and therapeutic applications. Because of the high surface area to volume ratio surface chemistry, and high density of defects, ferrite nanoparticle production has recently received greater attention [39,40].

Spinel ferrite nanoparticles such as $NiFe_2O_4$ have received a lot of attention for various applications, including high-frequency

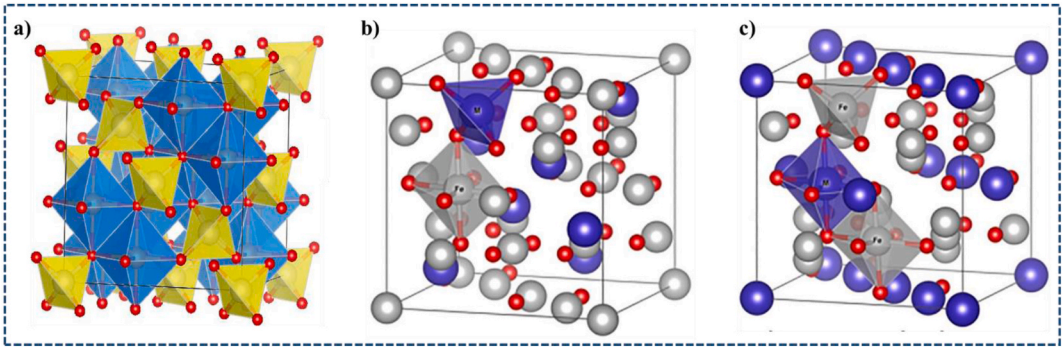

Fig. 1. Unit cell structure of magnetic spinel ferrite a) octahedral sites (blue), tetrahedral sites (yellow) and oxygen atoms (red) [30], b) normal spinel ferrite, and c) inverse spinel ferrite [31].

circuits, the cores of radiofrequency transformers, antennas, inductors, and radar-absorbing materials, due to their high resistivity and low loss at high-frequency [41]. They also have a lot of potential as catalysts and/or catalytic supports for degrading organic and inorganic contaminants. By combining their magnetic properties, antimicrobial activity, and hyperthermia therapy of cancer, $NiFe_2O_4$ NPs are becoming increasingly relevant in biomedical applications such as magnetic resonance imaging (MRI), drug delivery systems, and hyperthermia treatment of cancer [42,43]. Recently, research on $NiFe_2O_4$ NPs has attained considerable attention because of the differences in their physical and chemical properties from those of free atoms or molecules as well as those of bulk solids, and have a wide range of potential applications [44,45].

Ferrites play an important part in practically all electronic sectors due to their unique electromagnetic properties. Hard and soft ferrites are the two main types of ferrites. Manganese ferrite ($MnFe_2O_4$) is among the most fascinating soft ferrites. It has been extensively used in a range of applications over the past 50 years and has strong magnetic permeability and low losses. Magnetic resonance imaging (MRI), drug delivery, electronic devices, and several telecommunications divisions are among them. Compared to other spinel ferrites, manganese ferrite has a low resistance. The formula can be expressed as $[Mn_{1-i}Fe_i]$ (Mn_iFe_{2-i}) O_4, where brackets and parenthesis indicate the inclusion of a degree of inversion (i) [46].

However, it is well known that the method used to make ferrites could change the degree of inversion of the crystal structure. It has shown that the preparation methods such as sol-gel can change the magnetic behavior of zinc ferrite nanoparticles [47]. It implies that the cation distribution can affect the chemical and physical characteristics of spinel ferrite nanoparticles.

Mixed spinel ferrites such as, $CoMgFe_2O_4$, $CoZnFe_2O_4$ and $MgZnFe_2O_4$ are another important family members of magnetic ferrites that are studied due to their outstanding properties like high electrical resistivity, chemical stability, and high Curie temperature [48–50].

1.2. Magnetic properties

Nano-sized magnetic materials, with great interest have received a lot of attention due to the increased demand for miniaturized technological devices. Understanding magnetic properties at the nanoscale is critical for improving permanent magnetic material performance. As is widely known, the shape, size, surface effects, magnetic anisotropy, and other parameters have a significant impact on the magnetic properties of nanoparticles [51].

Hysteresis is a dampening phenomenon in which two related quantities, such as strain and stress, magnetic field, and magnetic induction, lag behind or get out of phase. The word “hysteresis” is derived from the Greek language and means “to lag behind.” Lattice heating is a result of some properties, such as magnetic and mechanical ones, being energy dampened. Magnetic and mechanical hysteresis is the most well-known forms of dampening [51]. Any magnetic circuit with ferromagnetic material will typically exhibit the hysteresis phenomena. The delay between changes in the magnetic flux density in this material and changes in the magnetic field strength is what causes these phenomena. Although the hysteresis mechanism is well understood, creating an appropriate mathematical model based on an understanding of the phenomena that explain the magnetization process is still a difficult issue. As a result, extensive research has been conducted over many decades to create a hysteresis model that is accurate and helpful in the field computations of ferromagnetic materials [52]. Measurements of hysteresis loops in technologically essential magnetic structures have revealed significant discrepancies from several fundamental and widely accepted ferromagnetism physics concepts [53]. In spinel ferrites, oxygen ions control the magnetic interactions between the spins of metallic cations in the octahedral and tetrahedral interstitial sites. Spin interactions with the exchanging of nearby atoms cause spinel ferrites to become magnetic. They are three different varieties of J_{AA} (A-*O*-A), J_{BB} (B– O–B), and J_{AB} (A–O–B) are governed by the superexchange process. The distance between the metallic ions and the oxygen affects the magnitude of these interactions. In comparison to A-*O*-A and B–*O*–B interactions, the A-*O*-B superexchange interaction is more significant.

The dominant intra-lattice negative J_{AB} interaction induces an uncompensated antiferromagnetic order (i.e., ferrimagnetism) between the A and B sub-lattices. The magnetic moments of the divalent cations at the B sites are the only ones responsible for the net moment in an inverse spinel structure because the contribution of the iron cations at B sites cancels that of the iron cations at A sites. The magnetic moments of the iron ions at the B sites are located in an antiferromagnetic alignment in a normal spinel. The difference between the contributions of two average sub-lattice magnetic moments can be used to calculate the magnetization of spinel ferrite.

Then the resultant saturation magnetization (M_S) of the ferrite at T = 0 can be expressed as follows:

$$Ms = \frac{N.d}{M_M}\left[\sum n_{B,B} - \sum n_{B,A}\right]\mu_B = \frac{N.d}{M_M}\mu_{eff}$$

where M_M refers the molar mass of ferrite, d is its density, N represents Avogadro’s number, and $n_{B,i}$ denotes the number of Böhr magnetons, μ_B, associated with the i site of the unit cell.

Magnetocrystalline anisotropy is a property of a magnetic material that defines the most energetically favorable crystallographic direction that spontaneous magnetization tends to align. For spinel ferrites, the magnetization axis direction is the stacking direction [111] of the close-packed arrangement but cobalt ferrite is not suitable for high permeability applications due to its significant magnetocrystalline anisotropy and high Co concentration. The magnetic characteristics of spinel ferrites not only depend on the composition of the ferrites but also on the choice of dopants and synthesis conditions that can affect the magnetic structure of spinel ferrites. As a consequence, the physical properties of magnetic spinel ferrites like magnetic saturation, coercivity, magnetic anisotropy, and magnetostriction are mediated by intrinsic magnetic properties of elements of composition. The spinel ferrites with high magnetic saturation that the researchers showed are based on Ni, Mn, Mg, Co, Li, and Cu.

Prasad et al. [54] synthesized nanocrystalline ferrites MFe_2O_4 (M = Zn, Ni, Cu, and Co) using auto-combustion process. Among all prepared spinel ferrite, $CoFe_2O_4$ had the highest saturation magnetization of 41 emu/g, whereas $ZnFe_2O_4$ showed a low saturation magnetization value of 12.87 emu/g (Fig. 2a).

Mohamed et al. [55] reported the saturation and coercivity values of $ZnFe_2O_4$ which rely on the cobalt doping ratio. By replacing Zn^{2+} ions with Co^{2+} the particle size of ferrite increased from 8.3 nm to 11.4 nm with an increase in the Co^{2+} doping content. The study revealed that the saturation magnetization value increased as the Co2+ content increased, from 40 emu/g when x = 0.0–98 emu/g when x = 0.4. The magnetic anisotropy significantly changed when the Co^{2+} content of the $ZnFe_2O_4$ host lattice increased (Fig. 2b).

The impact of Cu^{2+}, Ni^{2+}, and Co^{2+} substitution on the structural and magnetic characteristics of $Li_{0.25}Mn_{0.5-x}MxFe_{2.25}O_4$ spinel ferrites was reported by Mazen et al. [56]. The results showed the synergistic effect of replacing Mn^{2+} ions with Co^{2+} ions in enhancing the magnetic characteristics of Li–Mn ferrites (Fig. 2c).

Purnama et al. [57] studied the impact of calcination temperature on crystallite size magnetic properties of $CoFe_2O_4$ synthesized by co-precipitation process. It can be observed that as minor Co^{2+} and Fe^{3+} ions migrate between tetrahedral and octahedral sites, the saturation magnetization values increase. In addition, it was determined that the rise of the magnetic domain size, which promotes magnetization, was the explanation for how magnetization increased with particle size (Fig. 2d).

The magnetic properties, such as the inversion degree parameter, which are sensitive to the local structure, can be determined using a variety of element-specific techniques, such as Extended X-ray Absorption Fine Structure (EXAFS), X-ray Absorption Near Edge Structure (XANES), Diffraction Anomalous Fine Structure (DAFS), and X-ray Magnetic Circular Dichroism (XMCD). Mössbauer spectroscopy is another important characterization technique used to characterize magnetic properties and determination of inversion degree of spinel ferrites. This characterization method is used to determine the hyperfine connection between the iron nucleus and the electronic charge of the nearby atoms. For this reason, the preparation methods, particle size, shape, and calcination temperature must be taken into consideration for the preparation and application of spinel ferrites.

1.3. Synthesis methods

The manufacture of magnetic nanoparticles, which are commonly utilized in composite materials, involves two steps; first, the

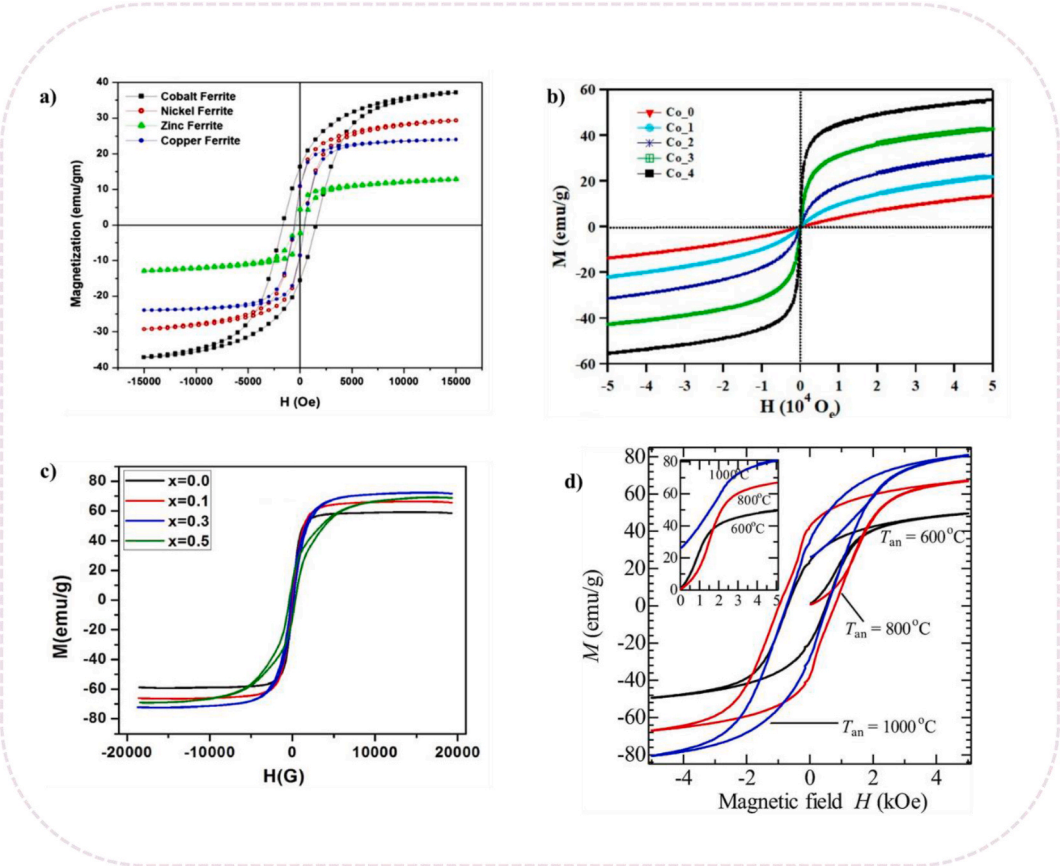

Fig. 2. Magnetization-filed (M–H) typical hysteresis curves. a) MFe_2O_4 (M = Zn, Ni, Cu, and Co) [54], b) $Co_xZn_{1-x}Fe_2O_4$ ferrite [55], c) $Li_{0.25}Mn_{0.5-x}Co_xFe_{2.25}O_4$ [56] and d) Co-precipitated $CoFe_2O_4$ nanoparticles at various calcination temperatures (600 °C, 800 °C and 1000 °C) [57].

synthesis of magnetic nanoparticles, and second, the modification of surface functionalities. Different processes can be utilized simultaneously to produce nanoparticles of various sizes. It is known that the synthesis process affects the physical and chemical behavior of nanoparticles. The development of new preparation techniques and application scenarios has been a key area of research since the discovery of magnetic nanoparticles. The most widely utilized techniques for creating magnetic nanoparticles nowadays are physical and chemical ones [58,59].

On the controlled synthesis of various sizes, compositions, and morphologies of magnetic nanoparticles, numerous synthesis approaches have been explored in the literature [42,60]. Among the various methods available for the synthesis of spinel ferrite materials, the most popular include physical, chemical and biosynthesis methods that will be the focus of this section. Table 1 summarizes some preparation methods of spinel ferrite nanoparticles.

1.3.1. *Chemical methods for preparing magnetic nanoparticles*

Chemical synthesis is the most common approach for preparing NPs since it has a high capacity for producing nanoparticles in a reasonable time and at a low cost. To date, several methods for preparing magnetic nanoparticles have been suggested and effectively used to fabricate a variety of magnetic nanoparticles. Based on the solvent used, all of these synthetic processes can be classified into two categories in terms of cost, size, and shape controllability: aqueous solvents and non-aqueous solvents. Aqueous-based magnetic nanoparticles are inexpensive, but it is difficult to control their shapes and sizes. Non-aqueous procedures are more expensive than aqueous ones but have more control over size and shape [68,69].

The main focus of this section is to introduce and review the conventional methods that are used to synthesize the spinel ferrite NPs with the general formula MFe_2O_4.

1.3.1.1. Co-precipitation. Co-precipitation is a simple and cost-effective process for the synthesis of MFe_2O_4 NPs. The spinel ferrite NPs synthesized by this method is homogeneous in structure, highly pure, and of controllable size [70]. In this method, solution of stoichiometric quantities of metal salts (chlorides, nitrates or sulphates) is mixed at sufficient temperatures with a base, which acts as a precipitating agent. Multiple factors such as temperature, pH, reaction time, as well as the type and the ratio of precursors play a significant role in controlling the size, shape, and properties of spinel ferrite NPs [71,72]. equation (1) describes the mechanism involved in the co-precipitation method for the synthesis of ferrite NPs [73]:

$$2M_A^{3+}\,(aq) + M_B^{2+}\,(aq) + 8OH^-\,(aq)\; M_AM_{B2}O_4\,(s) + 4H_2O \tag{1}$$

The spinel ferrites prepared by this process are homogenous in structure, very pure, and of controlled size. Co-precipitation is a traditional way of producing MFe_2O_4 MNPs for chemical synthesis in this regard. This method can be used to disperse huge volumes of MNPs in aqueous media with ease. Using this method, the precursor elements co-precipitate in a solution at high or room temperature after the base addition in an inert atmosphere. The ability to scale up and achieve huge amounts of MFe_2O_4 MNPs is one of the most important advantages of the co-precipitation approach. Co-precipitation is therefore the most typical chemical procedure used in industry to synthesize thousands of kilograms of MFe_2O_4 nanoparticles. However, the main challenges of the co-precipitation approach are morphological control, crystalline quality, and particle size distribution of MNPs [58,68]. The low crystallinity of NPs prepared with co-precipitation is the main difficulty associated with this method which can be improved with subsequent heat treatment [23].

$CoFe_2O_4$ nanoparticles with a typical co-precipitation process and a particle size range of 16–26 nm are presented in Fig. 3a-c [62]. In this procedure, polar solvents are utilized to dissolve inorganic salts such as nitrate and chloride to form a homogenous solution as the starting materials. It should be noted that factors like temperature, pH, and salt concentration that are detrimental to crystal growth and particle aggregation can control the size and shape of nanoparticles. The solid mass is collected and washed after precipitation. After that, the hydroxides are calcinated to produce crystalline oxides.

1.3.1.2. Hydrothermal and solvothermal synthesis. To create crystalline MFe_2O_4 magnetic nanoparticles, hydrothermal and solvothermal syntheses use a variety of wet-chemical processes. High purity and controllable morphology of MNPs can be produced by simple and effective hydrothermal and solvothermal procedures. A nonaqueous solution, such as methanol, ethanol, or ethylene glycol, is used in solvothermal synthesis to dissolve the metal precursors under high pressure and at a moderate temperature. Hydrothermal synthesis refers to the synthesis through chemical reactions in an aqueous solution above the boiling point of water [74].

Table 1
Preparation methods of spinel ferrite nanoparticles.

Methods	Iron Source	Reaction Conditions	Solvent	Ferrite Nanoprticles	References
Sol–gel	$Fe(NO_3)_3.9H_2O$	150 °C	H_2O/citric acid	$ZnFe_2O_4$	[61]
Co-precipitation	$FeCl_3$	75 °C	H_2O	$CoFe_2O_4$	[62]
Thermal Decomposition	Fe (acac)3	300 °C	Benzyl ether	$CoFe_2O_4$	[63]
Microemulsion	Iron (III) 2-ethylhexanoate ($C_{24}H_{45}FeO_6$)	40 °C	Isooctane/H_2O	$NiFe_2O_4$	[64]
Hydrothermal	$Fe(NO_3)_3.9H_2O$	180 °C	H_2O	$CoFe_2O_4$	[65]
Sonochemical	$Fe(NO_3)_3.9H_2O$	Room Temperature	H_2O	$MnFe_2O_4$	[66]
Microwave Assisted Synthesis	$FeCl_2$	Room Temperature/800 W	H_2O	Titanium ferrite	[67]

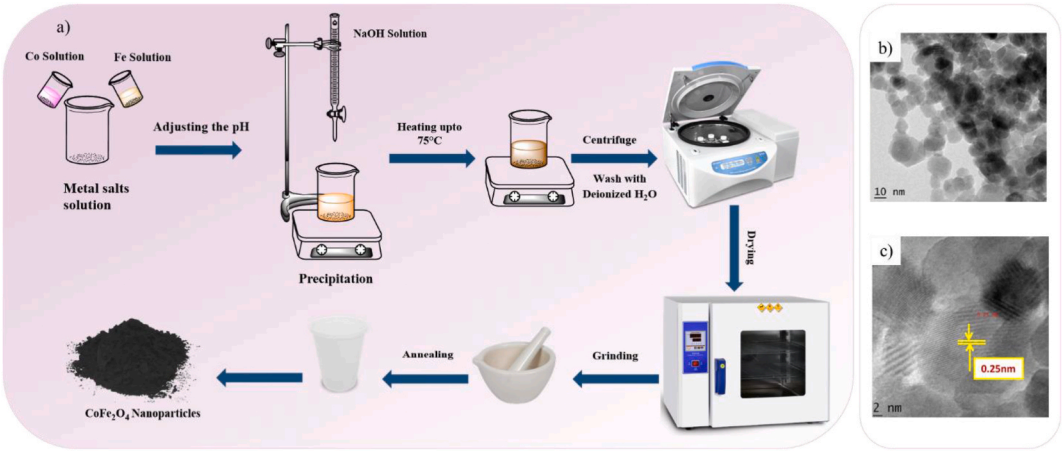

Fig. 3. a) Schematic diagram for the synthesis of $CoFe_2O_4$ NPs via co-precipitation technique, b) TEM image and c) HRTEM image of $CoFe_2O_4$ NPs [62].

Fig. 4 shows a schematic of the hydrothermal method, which involves using high-pressure reactors or autoclaves to achieve high pressures at high temperatures with control over size and shape and without the use of post-annealing treatment [65]. In this method, aqueous or non-aqueous solutions are used at high temperatures and high pressures to prevent the formation of dislocations in single-crystal magnetic nanoparticles. As a result, this approach can be used to create unstable crystalline phases around their melting point. In addition, this process allows for the creation of magnetic nanoparticles with high vapor pressure at their melting points while preserving good control over the compositions. This approach is particularly useful for creating hollow and controlled-shape spinel ferrite particles such as nanoflowers and cubic [75–77]. It should be highlighted that the synthesis temperature has a significant impact on the reaction kinetics and nucleation rate of this approach [68,78,79].

It is generally known that the properties of reagents, such as their solubility and reactivity, can alter at high temperatures. As a result, these changes offer more options for producing various morphologies and phases, such as metastable ones, which aren't possible at low temperatures. Therefore, this strategy has been widely used to produce a variety of target ferrites that are extremely pure and crystalline. According to this viewpoint, one advantage of this approach is that particle size, morphology, and other physical properties may be influenced by adjusting reaction temperature, time, dopants, and other variables [80].

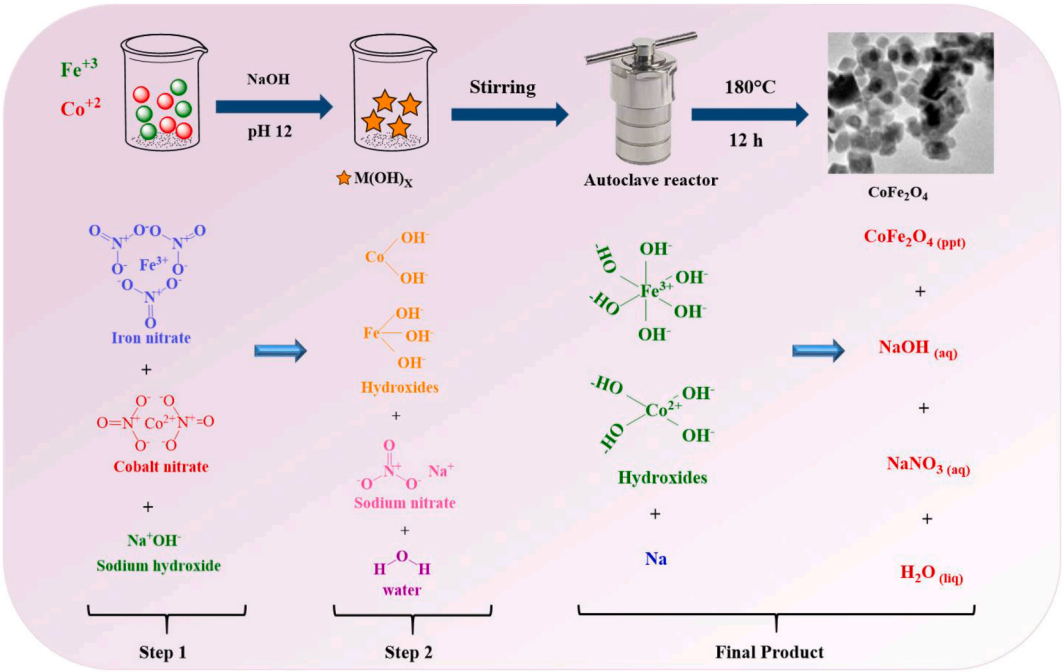

Fig. 4. Schematic representation of the hydrothermal reaction procedure [65].

1.3.1.3. Microemulsion. Microemulsions are clear, isotropic mixtures of water, oil, and a surfactant that are stable and clear. This method uses surfactants to aid in the coexistence of two immiscible liquids in a single phase. One of the microemulsion solvents is water/oil, which is used to prepare the solution by dispersing immiscible solvents [81]. The two most popular microemulsion methods for the synthesis of magnetic nanoparticles are reverse, in which water disperses in oil (w/o), and direct, in which oil disperses in water (o/w).

The water-in-oil microemulsion method for the synthesis of spinel ferrite NPs is illustrated schematically in Fig. 5a. A monolayer molecule having an oil-soluble hydrophobic head and a water-soluble hydrophilic tail, or the opposite could be utilized as a surfactant. The surfactant is employed to keep the solution stable, for instance, dodecyl sulfate. The magnetic nanoparticles precursor is typically dispersed as 1–100 nm nanodroplets in the aqueous phase. Surfactant molecules encircle water droplets, forming "micelles" that act as nanoreactors. This results in the formation of magnetic nanoparticles inside the micelles, which confines the particles and limits particle nucleation, development, and agglomeration. Finally, a second emulsion is added to the solution to precipitate the nanoparticles. For instance, in an attempt to produce nickel ferrite and zinc ferrite NPs as photocatalyst for water splitting, these NPs were synthesized using the oil in water microemulsion which allowed the synthesis of spinel ferrite NPs with sizes below 20 nm (Fig. 5b and c)(Table 1) [64].

The advantage of this method is that it is simple to adjust the size of MFe_2O_4 MNPs by size-modulating the particles to sub-nanometer sizes. The microemulsion method, on the other hand, produces a wide range of shapes and size distribution. This MFe_2O_4 MNP synthesis method has a low yield and a narrow working window when compared to other methods. Various studies, on the other hand, have yielded encouraging findings for scaling up the procedure for an economic or environmental facility [58,68,82].

1.3.1.4. High-temperature thermal decomposition. The thermal decomposition method overcomes the size and morphological constraint of the co-precipitation method. In general, the size distributions of magnetic nanoparticles produced at higher temperatures are more homogeneous. Additionally, more crystalline MFe_2O_4 MNPs can be synthesized by high-temperature decomposition. The thermal decomposition process of $CoFe_2O_4$ nanoparticles is schematically demonstrated in Fig. 6a. The fundamental advantage of this approach over co-precipitation is the separation of nucleation and growth phase of nanoparticles, resulting in monodisperse magnetic nanoparticles with a narrow size distribution, uniform morphology and a high crystalline structure [83]. Without the use of size selection methods, monodisperse magnetic nanoparticles can be made. Fig. 6b and c shows TEM images of the $CoFe_2O_4$ NPs with uniform size and average particle size of 13.2 nm and 9.3 nm derived via thermal decomposition process method [63].

In this method, the size and shape of spinel ferrite NPs can be adjusted by temperature, heating rate, the concentration of organic solids and type of organic solvent to make diverse shapes, such as cubic, and octahedral [84,85]. For biomedical applications of spinel ferrite NPs, thermal decomposition is preferable to the co-precipitation synthesis method due to high crystallite and narrow size distributions [86].

1.3.1.5. Sol-gel and sol-gel auto combustion. The sol-gel method, illustrated schematically in Fig. 7a, has been widely used to create

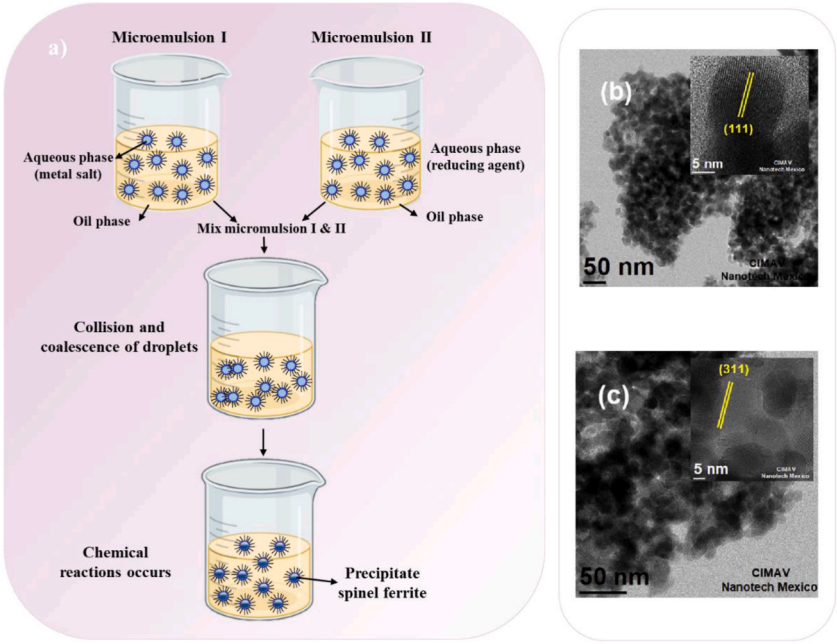

Fig. 5. a) Schematic diagram for the synthesis of spinel ferrite NPs via microemulsion process, TEM and HRTEM images b) nickel ferrite and c) zinc ferrite [64].

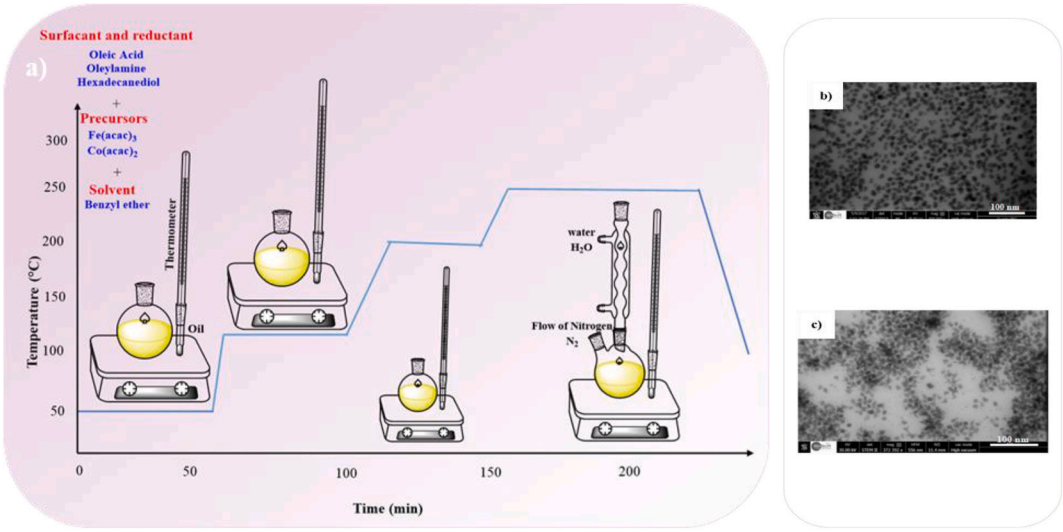

Fig. 6. a) Illustration of thermal decomposition method, STEM images of $CoFe_2O_4$ NPs b) d = 13.2 nm and c) d = 9.3 nm [63].

MFe_2O_4 MNPs with nanostructures for engineering applications due to the possibility of shape and size control [87]. Sol-gel procedure is a simple and low cost method, however, lack of purity of final product is the main limitation of sol-gel method that thermal treatment is needed to achieve the high purity and crystalline nanomaterials [88,89]. The shape and crystallinity of the nanoparticles produced by this method are significantly influenced by the type of precursors that were present in the initial colloidal solution.

In this method, the precursor solution is added to polymerization or hydrolysis reactions, which result in the production of sol. The gelation process makes use of polymer addition or sol condensation to gel then simple solvent evaporation is used to prepare MFe_2O_4 NPs. The main advantages of this method over alternative strategies include simple experiment setup, low temperature, and highly controlled synthesis [58,68]. Ferrite nanoparticles can be prepared using the sol-gel auto-combustion synthesis method, which combines chemical sol-gel and combustion processes [90]. This process uses an exothermic, self-sustaining, thermally-induced anionic redox reaction of xerogel, which is made from an aqueous solution containing the desired metal salts and an organic complexant such as urea, glycine, or citric acid. The temperature of the flame during combustion may range from 600 to 1350 °C [91,92]. The advantages of using sol-gel combustion are based on good chemical homogeneity, a highly pure and crystalline product, fine particle size, as well as easy control of stoichiometry of the final spinel. By adjusting the reactants ratio, pH, reaction conditions, and heat source, various shapes of ferrites such as nanospheres, hollow nanocages, and nanorods can be synthesized [90]. Fig. 7b and c shows TEM images of the Cu-ferrite with uniform size and average particle size of 56 nm and Zn-ferrite with average particle size in the range of 10–50 nm derived via sol–gel combustion and sol-gel methods, respectively [61,93].

1.3.1.6. Electrochemical method. The essential concept behind an electrochemical synthesis is the transfer of an electric current

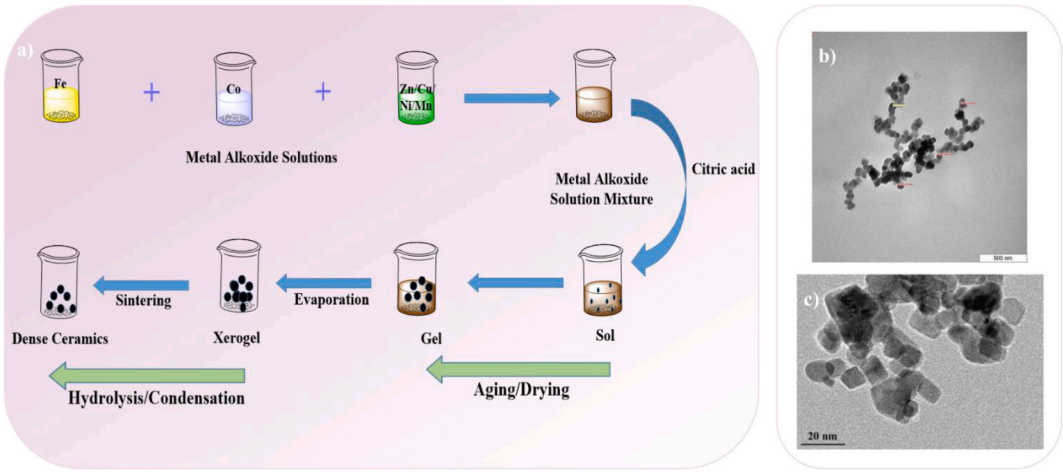

Fig. 7. The synthesis of spinel ferrite and transition metals-substituted spinel ferrite nanoparticles via sol-gel technique [87], b) $CuFe_2O_4$ via sol-gel combustion method [61], c) $ZnFe_2O_4$ NPs via sol-gel method [93].

between two or more electrodes (anode and cathode) situated in an electrolyte. With this technique, the anode can produce metal ion species in the electrolyte, which the cathode then reduces to a metal with the assistance of stabilizers [94]. Fig. 8a illustrates the main plan for the electrochemical production of $ZnxFe_{3-x}O_4$ferrite nanoparticles. For the synthesis of Mn, Co, and Ni ferrites Ovejero et al. [95] used an electrochemical method for synthesis (Fig. 8b and c). According to the literature, changing the deposition potential and electrolyte composition significantly affects the film-forming properties of magnetic nanoparticles [58].

1.3.1.7. Sonolysis or sonochemical methods. Sonolysis or sonochemical methods make use of high-intensity ultrasound irradiation to take advantage of the chemical reactions caused by sonic cavitation in order to formation of unique metal ferrite magnetic nanoparticle structures [97–100]. The ultrasonic irradiation causes bubbles that are constantly compressed and expanded, causing the bubbles to oscillate. The ultrasonic energy accumulates in the pulsating bubbles, which gradually grow until the bubbles collapse, releasing the accumulated energy. When the bubbles rupture, a highly localized energy burst takes place that swiftly and significantly raises temperature and pressure [101].

The sonolysis or sonochemical technique, albeit promising for fabricating magnetic nanoparticles with outstanding magnetic saturation properties, suffers from the synthesis of magnetic nanoparticles with a narrow size distribution. The magnetic nanoparticles synthesized by this technique are often amorphous, porous, and aggregated [68,102]. Yadav et al. [103] reported that the average crystallite sizes of $MnFe_2O_4$ NPs increased from 1.8 nm to 22.1 nm as the sonication period increased from 20 min to 80 min. Fig. 9 a, b show the schematic illustration and TEM image of the sonochemical synthesis of $MnFe_2O_4$ NPs at sonication time 80 min. Spherical shape $Zn_{0.35}Fe_{2.65}O_4$ nanostructures with an average size of 10–40 nm were successfully synthesized by PEG-6000 as a surfactant via the sonochemistry method and calcinated at 500 °C for 2 h (Fig. 9c) [104]. In another research, Er^{3+} and Dy^{3+} co-doped MnZn spinel nanoferrites were fabricated via ultrasonic irradiation. TEM image of spinel ferrites of $Mn_{0.5}Zn_{0.5}Er_xDy_xFe_{2-2x}O_4$ (x = 0.06) revealed the aggregation of small nanoparticles with an average diameter of 50 nm (Fig. 9d).

1.3.1.8. Microwave-assisted synthesis. Electromagnetic waves with frequencies ranging from 0.3 to 300 GHz and wavelengths between 1 mm and 1 m are known as microwaves. The typical frequency for microwave heating in labs and houses is 2.45 and at this frequency, the energy is only 103–105 eV which is equal rotational energies of molecules [106]. In general, microwaves heat all substances that have mobile electric charges, such as polar molecules in a solvent or conducting ions in a solid or a liquid. Heat is produced by the rotation, friction, and collision of molecules in polar solvents like water, which oscillate with the rapidly changing alternating electric field. Molecules lose energy in collisions with other solvent molecules [107]. The use of microwave heating in chemical processes is significantly faster, cleaner, and more cost-efficient than the conventional methods, and increasing the rate of chemical reactions between different metallic salts has made this approach a powerful method for creating magnetic nanoparticles with improved quality and properties. The microwave-assisted technique has been regarded as an environmentally friendly way to the synthesis ferrite nanomaterials with controllable shape and size [67,68,108]. Microwave-assisted synthesis has a number of advantages, one of which is the ability to produce metal ferrite magnetic nanoparticles with different phases and coating, which are desirable for many applications, including biological ones. Furthermore, the microwave-assisted approach may produce magnetic nanoparticles with great colloidal stability that can be distributed easily in water without the need for expensive and time-consuming purification and ligand exchange operations. For the mass manufacture of magnetic nanoparticles, these capabilities have made microwave-assisted synthesis competitive with thermal decomposition [68].

Magdalane et al. [109], developed the synthesis of porous $CoFe_2O_4$ and TiO_2 doped $CoFe_2O_4$ nanoparticles using *L-Threonine*as a fuel by microwave irradiation method and applied for photocatalytic degradation of organic dyes.

Titanium ferrite magnetic nanomaterials were fabricated by microwave radiation and the impact of titanium and microwave time

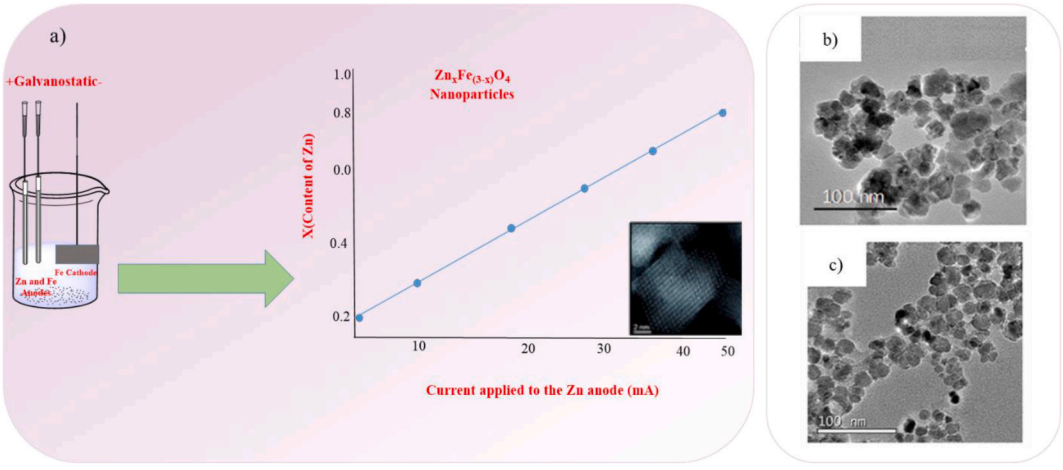

Fig. 8. a) Schematic diagram for the synthesis of metal ferrite NPs via electrochemical method [96], TEM images b) $MnFe_2O_4$ NPs, c) $NiFe_2O_4$ NPs [95].

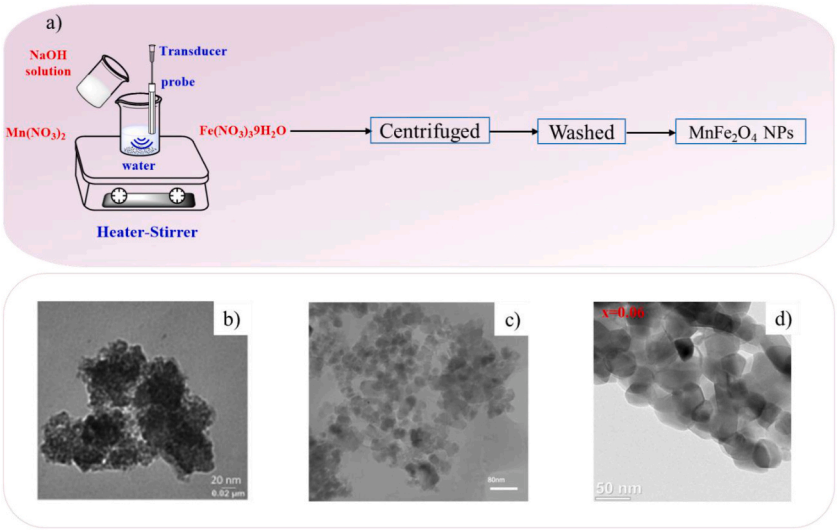

Fig. 9. a) Schematic diagram of sonochemical process and TEM images b) $MnFe_2O_4$ NPs [103], c) $Zn_{0.35}Fe_{2.65}O_4$ nanostructures [104] and d) $Mn_{0.5}Zn_{0.5}Er_xDy_xFe_{2-2x}O_4$ (x = 0.06) spinel nanoferrites [105].

on structural, optical and magnetic properties were investigated. The magnetic measurements of synthesized nanomaterials revealed that their magnetic properties enhanced as the titanium precursor or microwave radiation time increased. The microwave method for synthesize of titanium ferrite magnetic NPs is schematically demonstrated in Fig. 10a. TEM image of these ferrite nanoparticles showed that spherical nanoparticles have a tendency to form strong aggregation due to their magnetic nature (Fig. 10b)(Table 1) [67].

In another study, photocatalyst NPs of nickel-doped cobalt ferrite ($Ni_{0.5}Co_{0.5}Fe_2O_4$) were synthesized using a microwave-assisted method. The TEM image of $Ni_{0.5}Co_{0.5}Fe_2O_4$ NPs showed spherical and agglomerated particles (Fig. 10c) [110].

1.3.2. Biosynthesis

Biosynthesis of spinel ferrite nanoparticles using microbial enzyme or a plant phytochemical with stabilizing and/or reducing properties as an environmentally friendly method is an emerging research area and a suitable alternative to chemical and physical methods [111–114](Fig. 11a). Magnetotactic bacteria and iron-reducing bacteria have traditionally been utilized to synthesize metal ferrite magnetic nanoparticles. This method has shown potential in increasing the magnetization properties of metal ferrite NPs by doping them with cobalt. The phase of the produced magnetic nanoparticles is determined by the species of bacteria and the preparation circumstances (aerobic or anaerobic). *Actinobacter* bacteria, for example, can be used to synthesize maghemite nanoparticles with superparamagnetic properties in an aerobic environment [115]. Since the mechanism of magnetic nanoparticle biogenesis is generally poorly understood, it is challenging to pinpoint the variables that control shape and size while maintaining the proper saturation magnetization [68].

Chuita et al. used a convenient green process for the synthesis of biogenic $CuFe_2O_4$ magnetic nanoparticles using tea extracts with an average size of 8.78 nm (Fig. 11b) [116]. In another study, $NiFeFe_2O_4$ NPs were synthesized by a green method using *Hydrangea paniculata* flower extract with a size range10–45 nm (Fig. 11c) [117]. This approach has various benefits, including a shorter processing time, homogeneous nanomaterial size and morphology, and mild reaction conditions. However, this approach has numerous

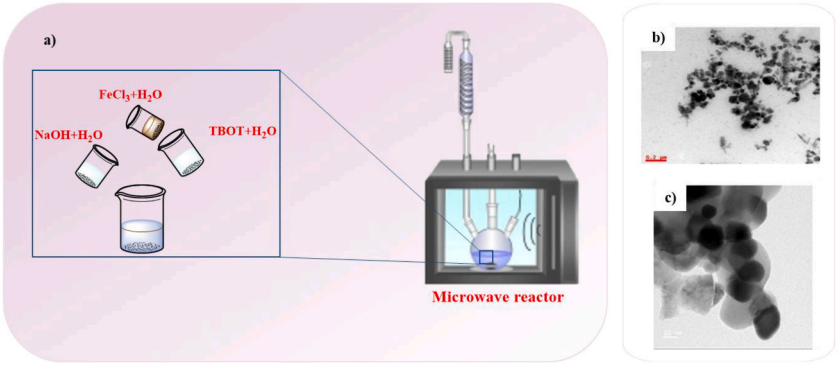

Fig. 10. a) An illustration of the experimental setup used for the synthesis of titanium ferrite magnetic nanomaterials by microwave method, TEM images b) titanium ferrite magnetic NPs [67] and c) $Ni_{0.5}Co_{0.5}Fe_2O_4$ NPs [110].

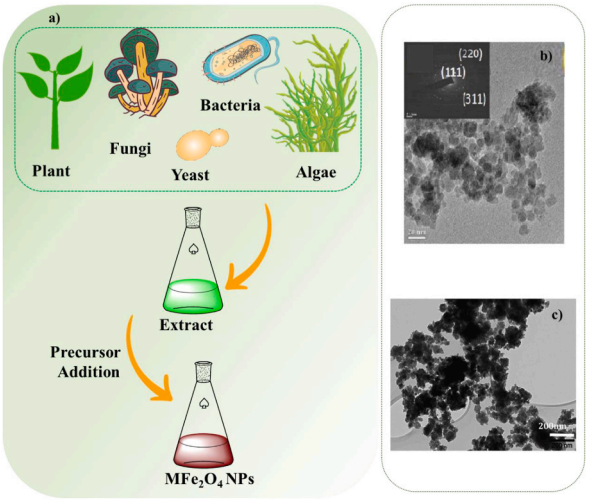

Fig. 11. a) Schematic biosynthesis of spinel ferrite nanoparticles, TEM images b) $CuFe_2O_4$ [116] and c) $NiFe_2O_4$ NPs [117].

limitations, including challenges with large-scale production, a low yield, and the coexistence of organic contaminants. To overcome these limitations, appropriate synthetic strategies must be used. Table 2 summarizes of magnetotactic bacteria employed for the preparation of metal ferrite nanoparticles as well as biological systems for the formation of metal ferrite nanoparticles.

1.3.3. Physical method

The majority of physical procedures used to break down a bulk spinel ferrite material into nanoparticles are top-down processes. Several well-known instances of physical techniques are electrical wire explosions and mechanical milling [123,124], and laser target evaporation [125–127]. Guo et al. [128], synthesized spinel ferrite $CoFe_2O_4$ NPs via laser ablation of the spinel ferrite $CoFe_2O_4$ target in the solution of Au NP colloidal solution and Au–$CoFe_2O_4$ NPs formed. Although physical methods offer better production yields (up to 200 g/h), they only produce around 10% of the magnetic nanoparticles needed for various applications [68]. This is due to the difficulty in controlling the shape and size distributions and the comparatively high power consumption of physical techniques. The earliest process to the synthesis spinel ferrite nanostructures is mechanical ball milling [38]. In this process, powders (such as oxides, carbonates, and other metal-containing compounds) are ground in high-energy ball mills, and the mixture is then heated to high temperatures to transform the mixture into the required phase of the materials.

The mechanical ball milling procedure is further divided into two types: dry and wet. A wet approach is a great option for producing high-magnetization crystal particles. Fig. 12(a-d) shows the dry and wet milling procedures before and after milling, respectively. The ball milling method is simple to use, however impurities can readily be added during the preparation stage, and mechanical and chemical factors can impact on the crystalline structure of MFe_2O_4. As a result, the mechanical ball milling process is ineffective for producing nano-MFe_2O_4 crystals of various morphologies [58].

1.4. Dopants

The properties and colloidal stability of spinel ferrite NPs can be altered by using adopting metals that is useful for the fabrication of MFe_2O_4 NPs in various applications. The physical and chemical properties of spinel ferrite including redox activity, thermal stability, and architectural stability are significantly influenced by the metals occupying its octahedral or tetrahedral positions. Rare earth ions (Ga, La, Sm, Gd, Dy) are common substations for the Fe site, while transition metals (Cu, Zn, Co, Ni, etc.) are typical substations for the M site [129]. Magnetic materials, such as ferrites, are cross-sectional powders and ceramic-based materials with ferromagnetic properties derived from iron oxides, the main constituents of which are Fe_2O_3 and Fe_3O_4, and which can also be doped with transition metals and metal oxide nanoparticles. Ferrites and metallic doped ferrites are magnetic materials that are used in various applications such as photocatalysis, drug delivery in cancer treatment, bioimaging, hydrogen production, and electronic expedients [130,131].

Table 2
Metal ferrite nanoparticles produced by microorganisms.

Microorganisms	Culturing temperature	Size (nm)	Shape	Location	References
Shewanella oneidensis	28	40–50	Rectangular, rhombic, hexagonal	Extracellular	[118]
Recombinant AMB-1	28	20	Cubo-octahedral	Intracellular	[119]
Yeast cells	36	Not available	Wormhole-like	Extracellular	[120]
Yeast cell	36	Not available	Nanopowders	Extracellular	[121]
Shewanella oneidensis MR-1	25	30–43	Pseudohexagonal/irregular or rhombohedral	Intracellular	[122]

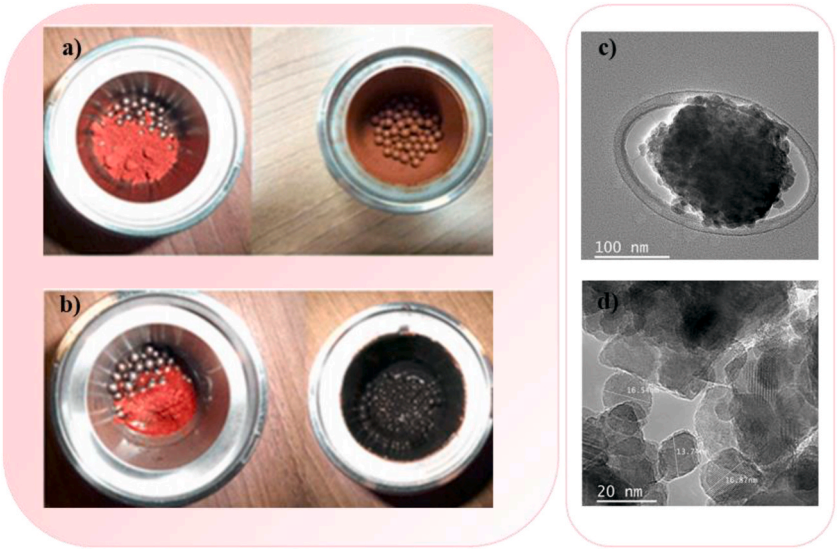

Fig. 12. Photograph of the milling materials a) Before and after dry milling and b) Before and after wet milling, TEM images c) dry milling and d) wet milling of iron oxide nanoparticles [58].

Due to their high surface area, which produces superior properties as compared to bulk materials, researchers have been interested in studying materials at the nanoscale level. The electrical, optical, and magnetic characteristics of spinel ferrite materials, which have a general formula of AFe_2O_4, are well known, particularly at the nanoscale scale. The main objective of doping ferrite nanoparticles with metal ions such as (Al^{+3}, Mn^{+2}, Ag^{+}, Y^{+3} etc.) was to enhance their physical and chemical properties. These properties are crucial for applications like photocatalysis in dye photodegradation and antibacterial agents, industrial uses, and electrochemical energy storage materials. Structure, optics, electricity, infrared radiation, and magnetic characteristics have all been proven to be impacted by doping [132].

Several papers describe the utility of metal ferrite magnetic nanoparticles doped with different elements and their applications in diverse fields in the literature. Therefore, this article review has selected numerous publications of doped spinel ferrites with transition metals and rare earth metals.

1.4.1. Transition metal substituted metal ferrite NPs

The magnetic properties of spinel ferrites can be altered by changing their chemical composition, for example by adding with transition metals (Zn^{2+}, Cu^{2+}, Co^{2+}, Mn^{2+}, Ni^{2+}, etc.). This can be result in improved performance and functionality of spinel ferrites in various applications. In spinel ferrite NPs, doping with transition metals can alter the moment of the NPs, which affects their magnetic properties such as magnetic susceptibility, coercivity, and remanance. When divalent metal ions such as Zn^{+2}, and other divalent metal ions are doped in metal ferrite, the structure of metal ferrite changes. Deepali et al. [133] studied the effect of Zn^{+2} doping on $CoFe_2O_4$ nanoparticles prepared via the co-precipitation method. They demonstrated that Zn^{+2} doping can yield particles with comparable shape, size, and structure while also exhibiting different magnetic anisotropy. It seems that the Hysteresis loop of $ZnFe_2O_4$ is very small as compared to $CoFe_2O_4$ which concluded that the zinc ferrite is soft magnetic material than the cobalt ferrite. However, the magnetic characteristics of cobalt ferrite decrease as Zn^{2+} substitution increases. Abdel Maksoud et al. [134], synthesized $Co_{1-x}ZnxFe_2O_4$ (x = 0–0.75) NPs using the sol-gel method. They claimed that the structure and morphology of NPs are significantly affected by the substitution of zinc ions. The increase of dopant resulted in a sharp reduction of saturation magnetization and remanence values. It also enhanced the magnetic and dielectric characteristics of NPs. The same strategy of Zn doping nanoparticles fabrication has been reported by Atif et al. [135]who applied the sol-gel process to study the impact of Zn doping on the magnetic and dielectric characteristics of cobalt ferrites $Zn_xCo_{1-x}Fe_2O_4$ (x = 0.00–0.60). They discovered that adding Zn^{+2} ions decreased coercivity and magnetostriction. Additionally, saturation magnetization reached its maximum (436.9 kA/m) at Zn = 0.4. Furthermore, low-frequency dielectric constant values were observed, suggesting that $Co_{0.6}Zn_{0.4}Fe_2O_4$ could be utilized as a stress sensor.

Melo et al. [65] investigated the preparation of Nickel-doped cobalt ferrite [$Co_{1-x}NixFe_2O_4$ ($0 \leq x \leq 1$)] nanoparticles with the hydrothermal method. They noticed Crystallite size was essentially spherical for lower nickel concentrations and diamond form comprised of nanosized grains for higher nickel concentrations, according to structural, morphological, and microstructural characterization. With the Ni^{2+} ions (x) concentration decreasing, the optical band-gap (E_g) values reduced to 2.94 and 2.51 eV for x = 0 and x = 1, respectively. The magnetic characteristics of cobalt ferrite were altered by the presence of nickel in the structure. They also discovered that the presence of nickel in the cobalt ferrite structure seemed to have an impact on its magnetic properties. For example, for x = 0 and x = 1, the saturation magnetization, Ms, and Mr, decreased from 369 to 256 emu cm^3 and 131–45 emu cm^3, respectively.

The effect of Al^{3+} doping on the on magnetic behavior of cobalt ferrite NPs investigated by Waghmare et al. [136]. They found that increasing the Al^{3+} concentration resulted in a decrease in the lattice constant and an increase in grain size (17.8–25.6 nm), which they

attributed to the impact of non-magnetic aluminum ions on grain size. Al ions replace Fe^{3+} in the B site during non-magnetic Al-doped cobalt ferrite, reducing the connection between A and B since Al ions are not involved in the exchange interaction. Saturation magnetization was reduced as a result of an increase in Al^{3+} content (0.85, 0.01 emu/g). As the concentration of Al^{3+} in cobalt ferrite increased, Hc decreased as the anisotropy field decreased, lowering the domain wall energy (550.52, 535.43 Oe). According to the researchers, this decline is due to a reduction in grain size.

Dou et al. [137] synthesized manganese-doped cobalt ferrite nanoparticles via sol-gel auto combustion method at a temperature of 400 °C and used for dye degradation. According to their findings, the obtained $CoFe_2O_4$ nanoparticles displayed ferromagnetic behavior at room temperature, with Ms and Mr 47.1emu/g and 27.5emu/g, respectively. The magnetism of the $CoMn_{0.2}Fe_{1.8}O_4$ sample has not decreased significantly, Although Ms and Mr decreased with the addition of Mn. This indicates that the Mn has been incorporated into the structure of cobalt ferrites, which was further validated by XRD patterns. Patil et al. [33] used a sol-gel auto--combustion method to synthesize Ti-doped $CoFe_2O_4$ nanoparticles with the formula $Co_{1+x}Ti_xFe_{2-2x}O_4$ (x = 0–0.5). They showed the formation of the cubic spinel structure of the samples with an average particle size of around 25 nm. They found that doping non-magnetic Ti^{4+} into $CoFe_2O_4$ nanoparticles allowed them to alter and optimize the magnetic properties of samples. At room temperature, the ferrimagnetic character of the nanoparticles was demonstrated using the hysteresis loop (M − H). According to magnetic properties, doping titanium ion from x = 0 to x = 0.5 reduced Ms from 83.08 emu/g to 51.86 emu/g and coercivity from 1339.85 Oe to 164.17 Oe. The structural, and magnetic properties of Ti-doped $CoFe_2O_4$ NPs made them ideal for nanoelectronics applications such as transducers, recording tapes, and magnetic data storage switching devices. Mund et al. [19] synthesized Mg^{2+}-substituted $CoFe_2O_4$ ($Co_{1-x}Mg_xFe_2O_4$, x = 0–1) NPs using the sol-gel auto-combustion technique. The saturation magnetization (72.96–35.22 emu/g) and coercivity (488.92–38.28 Oe) decreased as the dopant concentration increased from x = 0.2 to x = 1). Furthermore, doping Mg into $CoFe_2O_4$ modified the magnetic characteristics of the nanoparticles, converting the hard magnetic material to soft magnetic cobalt ferrite. As a result, increasing Mg content may lower Saturation magnetization and coercivity.

The effect of magnesium on magnetic properties of $Mg_{0.5}Zn_{0.5-x}Cu_xFe_2O_4$ (x = 0.0–0.5) ferrite nanostructures investigated by Zaki et al. [50]. According to their results, due to Cu^{2+} ions having a smaller ionic radius than zinc ions, the lattice constant decreased with increasing Cu^{2+} concentration. The magnetic properties of nanocrystalline ferrites were shown to be sensitive to particle size and surface area. At low frequencies and low temperatures, T ≤ 100 °C, the influence of Cu^{2+} substation on AC conductivity showed considerable behavior.

In another research study, Lin et al. [138] synthesized chromium-doped nickel ferrite $NiCr_xFe_{2-x}O_4$ (x = 0–1.0) particles via a sol-gel auto-combustion technique. The XRD revealed a single-phase spinel structure in samples with x > 0.2, indicating that a higher Cr^{+3} content in a sample is beneficial for the synthesis of chromium-doped nickel ferrite. With an increase in Cr^{+3} content, the lattice parameter decreased. $NiCr_xFe_{2-x}O_4$ Mössbauer spectra revealed two conventional Zeeman-split sextets with ferrimagnetic activity and also showed iron was in the Fe^{3+} form, and the magnetic hyperfine field at the tetrahedral tendency to diminish as the Cr^{+3} substitution increased. Along with the Cr^{3+} ions, the saturation magnetization reduced to Ms = 4.46 emu/g.

Table 3 summarizes the studies that have been done on transition metal substituted spinel ferrite NPs.

1.4.2. Rare earth metals substituted metal ferrite NPs

Physico-chemical characteristics of magnetic ferrite can be adjusted by substituting large size rare earth metal cations such as Eu^{3+}, Gd^{+3}, Nd^{+3}, Dy^{+3}, Y^{+3}, Yb^{+3}, In^{+3}, Pr^{+3}, Sm^{+3}, Tm^{3+}, Ho^{3+}, Er^{3+}, La^{3+}, and Ce^{2+}. This substitution results in significant strain, specific surface area changes and reduction in particle size. The synthesis method, type of rare earth dopant, type and concentration of dopant, heat treatment, processing and cation occupy on A and B sites all play a role in influencing the structural and magnetic properties of rare earth doped ferrite. Gadolinium substituted cobalt ferrite NPs ($CoFe_{2-x}Gd_xO_4$, 0 ≤ x ≤ 0.4) were prepared by hydrothermal method, showed a single phase cubic spinel structure when x ≤ 0.24 [152]. The effect of the yetterbium was studied by Virlan et al. [153]. Magnetic saturation risesed from 48.3 to 59.5 for x = 0.01–0.05, then falls to 34.2 for x = 0.3. Hc followed the same pattern, increasing from 845 (x = 0.01) to 985 (x = 0.05) and then decreasing to 658 (x = 0.3). The effect of Dy on the structural and magnetic properties of Mn_Zn ferrite NPs reported by Zipare et al. [154] The saturation magnetization decreased as Dy^{+3} concentrations increased, which could be linked to changes in the A-B exchange interactions as a result of structural changes caused by Dy^{+3}

Table 3
Preparation methods of transition metals substituted spinel ferrite NPs.

Metal ferrite NPs	Dopants	Preparation Method	References
$NiFe_2O_4$	Zn^{+2}	Sol-gel auto-combustion	[139]
$MgFe_2O_4$	Zn^{+2}	Sol-gel	[140]
$CoFe_2O_4$	Zn^{+2}	Co-precipitation	[141]
$SrFe_2O_4$	Ni^{+2}	Co-precipitation	[142]
$NiFe_2O_4$	Al^{3+}	Sol-gel auto-combustion	[143]
Ni–Mn–$CoFe_2O_4$	Al^{3+}	Sol-gel	[144]
Mn Fe_2O_4	Cu^{+2}	Solvothermal	[145]
Co Fe_2O_4	Cu^{+2}	Co-precipitation	[146]
$CoFe_2O_4$	Mn^{2+}	Sol-gel	[147]
Fe_3O_4	Mn^{2+}	Co-precipitation	[148]
Zn–$LaFe_2O_4$	Cr^{+2}	Sonochemical	[149]
Mg–Mn Fe_2O_4	Ag^{+}	Sol-gel	[150]
$NiFe_2O_2$	Ag^{+}	Co-precipitation	[151]

substitution. The Curie temperature of $Mn_{0.5}Zn_{0.5}Fe_2O_4$ NPs is 124 °C, and it drops to 84 °C as the Dy^{+3} concentration increased. As a result of Dy-substitution, the superexchange interaction between A-site and B-site weakens, resulting in a drop in Curie temperature. These samples seem to be appropriate for the development of temperature-sensitive ferrofluids for heat transfer applications due to their lower Curie temperature and greater thermomagnetic coefficient values. Cd substituted cobalt ferrite particles ($Cd_xCo_{1-x}Zr_{0.05}Fe_{1.95}O_4$) synthesized by sol-gel method and followed by calcination at the temperature of 700 °C. Saturation magnetization was reported to decrease from 67.89 to 57.33 emu/g while the coercivity reported to decrease from 1352 to 1120 Oe as Cd concentration (x) increased from 0 to 0.3 [155].

The research conducted in the rare earth application as a dopant for light and heavy groups is summarized in Table 4.

1.5. Applications of spinel ferrites

The main applications of MFe_2O_4 are illustrated in Fig. 13. The properties of ferrite, including its structure, particle size, and shape, can vary depending on the cation type and synthesis method employed, resulting in diverse applications.

1.5.1. Sensors

Sensors are electronic devices that detect changes in a given material in a specific environment. Ferrite nanoparticle-based sensors possess exceptional sensitivity, low detection limits, and high signal-to-noise ratios. The detection of variations in humidity is one of the most common uses of sensors. The monitoring of humidity is a widespread practice in both industrial and residential settings, as it helps to maintain human comfort, regulate storage conditions for various items, and ensure optimal operating conditions for industrial processes and devices. Typically, humidity sensing is primarily attributed to the surface effects of the interaction between water vapor and solids. Ceramic-based humidity sensors that utilize metal oxides have shown superior performance in terms of physical stability, thermal capability, mechanical strength, and chemical resistance compared to polymer films, making them a suitable choice for applications in electrochemical humidity sensors. The electrical properties of ceramic surfaces, such as resistance, capacitance, or

Table 4
The rare earth elements as a dopant in magnetic ferrites.

Metal ferrite NPs	Dopants	Preparation method	References
$CoFe_2O_4$	Eu^{3+}	Solvothermal	[156]
$CoFe_2O_4$	Eu^{3+}	Co-precipitation	[157]
$CoFe_2O_4$	Eu^{3+}	Precipitation & Hydrothermal	[158]
$BiFeO_3$	Eu^{3+}	Sol-gel	[159]
$BiFeO_3$	Eu^{3+}	Sol-gel	[160]
$CuFe_2O_4$	Eu^{3+}	Solution combustion	[161]
$BiFeO_3$	Eu^{3+} and Ni^{+2}	Sol-gel	[162]
$GaFeO_3$	In^{+3}	Solid- state reaction	[163]
Ni–$CoFe_2O_4$	In^{+3}	Co-precipitation	[164]
Mg–Ag–$MnFe_2O_4$	In^{+3}	Sol-gel auto-combustion	[165]
$CuFe_2O_4$	In^{+3}	Sol-gel	[166]
Cu–$NiFe_2O_4$	In^{+3}	Sol-gel auto -ignition	[167]
$CoFe_2O_4$	Pr^{+3}	Hydrothermal	[168]
$CoFe_2O_4$	Pr^{+3}	Sol–gel auto-combustion	[169]
$CuFe_2O_4$	Pr^{+3}	Sol-gel	[170]
$BiFeO_3$	Pr^{+3}	Sol-gel	[171]
Ni–Mn–$ZnFe_2O_4$	Pr^{+3}	Sol-gel	[172]
$ZnFe_2O_4$	Sm^{+3}	Co-precipitation	[173]
Ni–$CoFe_2O_4$	Sm^{+3}	Sol-gel	[174]
$BiFeO_3$	Sm^{+3} and Co^{+3}	Sol-gel	[175]
$BiFeO_3$	Sm^{+3} and Co^{+3}	Sol-gel	[176]
$NiFe_2O_4$	Sm^{+3}	Sol-gel auto combustion	[177]
Cu–$CoFe_2O_4$	Sm^{+3}	Citrate combustion	[178]
Mn–$ZnFe_2O_4$	Sm^{+3} and Gd^{3+}	Solution combustion	[179]
$CuFe_2O_4$	Tm^{3+}	Sol-gel	[180]
$NiFe_2O_4$	Tm^{3+}	Sol-gel	[181]
$CoFe_{2-x}Ho_xO_4$	Ho^{3+}	Solid state reaction	[182]
Cu–$ZnFe_2O_4$	Ho^{3+}	Sol-gel	[183]
Mn–$ZnFe_2O_4$	Ho^{3+} and Dy^{3+}	Solution combustion	[184]
$BiFeO_3$	Er^{3+}	Citrate-gel auto-combustion	[185]
$CoFe_2O_4$	Er^{3+}	Microemulsion	[186]
Cu–$CdFe_2O_4$	Er^{3+}	Citrate-gel auto-combustion	[187]
Co–$ZnFe_2O_4$	La^{3+}	Sol-gel	[188]
Zn–$CuFe_2O_4$	La^{3+}	Co-precipitation	[189]
$CoFe_2O_4$	La^{3+}	Co-precipitation	[190]
$CeFe_2O_4$	La^{3+}	Hydrothermal & Co-precipitation	[191]
Ni–$CuFe_2O_4$	Ce^{2+}	Co-precipitation	[192]
$MnFe_2O_4$	Ce^{2+}	Auto-combustion	[193]
Cu–Cd–$CoFe_2O_4$	Ce^{3+}	Co-precipitation	[194]

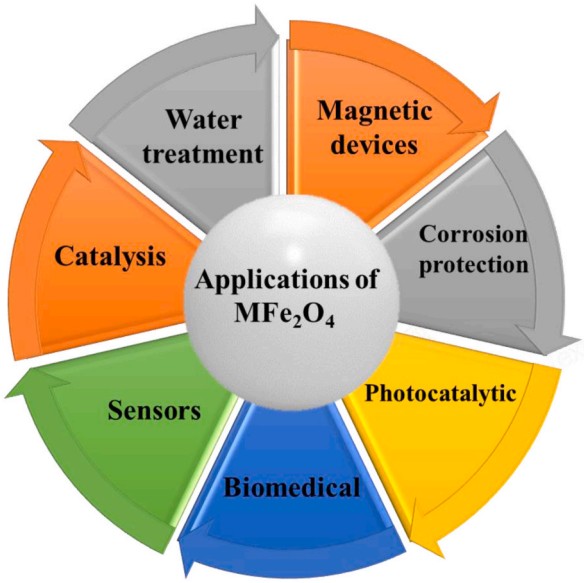

Fig. 13. Applications of MFe_2O_4.

electrolytic conduction, undergo changes due to the adsorption of water. In this case, when humidity rises, so does conductivity, resulting in a greater dielectric constant.

The microstructural properties of a material that are related to the synthesis procedure determine its humidity-sensing efficiency. $ZnFe_2O_4$ nanoparticles exhibit high sensitivity for humidity sensing, which can be attributed to their small grain size, large surface area available for water vapor adsorption, and low barrier height. Similarly, $CoFe_2O_4$, $CuFe_2O_4$, and $NiFe_2O_4$ nanoparticles have demonstrated effectiveness in sensing oxidizing gases like chlorine. $CoFe_2O_4$ sensors and actuators are more durable and widely used due to their high H_C values and stability. The combination of high magnetostriction, sensitivity to applied stress, chemical inertness, and low cost has sparked interest in the use of magnetostrictive $CoFe_2O_4$ composites for the development of magnetoelastic sensors. Additionally, due to its bifunctional nature in terms of stress sensing and actuation or contraction under the influence of a magnetic field, $CoFe_2O_4$ has been identified as a smart material with numerous technological applications in position sensors [195].

For application in gas sensos, ferrites with a single metal ion dopant, mixed ferrite materials (multi-ion doping), composites of ferrite with other metal oxides, polymers, and carbon materials/ferrite-based core-shell structures were also studied and Ranga et al. [196] summarized the findings in these results.

1.5.2. Photoluminescent applications

Mixed spinel nanostructures such as $CoFe_2O_4$, $NiFe_2O_4$, and $ZnFe_2O_4$ are known for their photoluminescence at room temperature, which is considered one of their most significant properties. The spectrum of photoluminescence offers insights into various characteristics such as surface oxygen vacancies, defects, charge carrier trapping, and transfer efficiency. The broad visible band emission in mixed spinel nanostructures such as $CoFe_2O_4$, $NiFe_2O_4$, and $ZnFe_2O_4$ is attributed to charge transfers among Fe^{3+} at octahedral sites, M^{2+} (M = Co, Ni, and Zn) at both tetrahedral and octahedral sites, and the surrounding O^{2-} ions. The blue emission peak at 460 nm is attributed to the Fe^{3+} transition at the ferrite sites, whereas the primary peak at 418 nm is attributed to the free electrons that are trapped at the oxygen vacancies. As the Ni content increased, the intensity of each peak decreased due to the rising bandgap, which reduced the electron-hole recombination ratio. Radiating flaws related to interface traps within grain boundaries caused the violet emissions. With increasing doping fraction, the luminescence intensity of Co^{3+} from $CoFe_2O_4$ decreases, implying a reduced electron-hole recombination ratio. The energy gap of nanocrystalline $ZnFe_2O_4$ was measured to be around 2.13 eV using photoluminescence [197].

1.5.3. Magnetic applications

The variation of exchange contact between tetrahedral and octahedral sites causes the magnetization to be dependent on grain size. To minimize media noise in high-density magnetic recording, the magnetic particles utilized should have a nanoscale size to limit the exchange interactions occurring between adjacent grains. To achieve great storage density, the particles must also have high H_C values. The magnetic characteristics (M_R, M_S, and H_C) of spinel ferrites are affected by their composition, particle size, crystal structure, and cationic distribution between octahedral and tetrahedral sites. Furthermore, they may exhibit antiferromagnetic, ferromagnetic, and paramagnetic behavior [198].

A rise in HC values in spinel ferrites can be attributed to a combination of factors, such as spin disorder, spin canting effect, and an increase in surface barrier potential in surface layers. The fascinating and improved properties of magnetic nanoparticles compared to similar bulk materials can be attributed to the large surface-to-volume ratio of the nanoparticles, which leads to the presence of a

significant number of atoms at the surface. Furthermore, the low number of coordination surface atoms in comparison to its interior atoms in nanoparticles results in different surface effects, such as spin canting, spin disorder, and the presence of a magnetically dead layer [199].

Materials possessing high coercivity are referred to as hard materials, whereas those with low coercivity are termed soft materials. Inductor cores, transformers, and microwave devices are made of soft materials, while permanent magnets are made of hard materials. In general, soft ferrites are characterized by a low coercivity value, and their magnetization can be adjusted, making them suitable for advanced electronic engineering purposes, such as transformer cores, high-frequency inductors, and microwave components [200].

1.5.4. Dielectric applications

The dielectric structure typically consists of grains that are good conductors separated by grain boundaries with low conductivity. The dielectric properties of spinel ferrites are influenced by factors such as structural homogeneity, cation distribution, particle size, density, and porosity. Additionally, the dielectric properties can be significantly affected by synthesis techniques and thermal treatment parameters such as temperature, time, and heating/cooling rates.

The presence of a small Co^{2+} ion at the tetrahedral site in $CoFe_2O_4$ results in a lower lattice constant, facilitating electron hopping between Fe^{3+} and Fe^{2+} ions and acting as a source of charge carriers, leading to an increase in the dielectric behavior of $CoFe_2O_4$. The polarization in $CoFe_2O_4$ is determined by the low-frequency hopping of charge carriers, which accumulates and causes polarization when it reaches the grain boundaries, resulting in high dielectric constants. The synthesis method and thermal treatment factors such as temperature, time, or heating and cooling rate play a significant role in determining these properties. The hopping of charge carriers at higher frequencies, on the other hand, is unable to follow the alternating current-produced field and is thus incompletely polarized, resulting in low dielectric constants. The dielectric constant falls as grain size increases, resulting in a smaller grain boundary between the microscopic grains. Lower frequencies have a large dielectric constant, which lowers as frequency increases. At a certain frequency, the decrease in dielectric constant becomes stable since at higher frequencies, only the dielectric polarization is responsible for contributing to the dielectric constant. At low temperatures, the charge carriers have limited mobility and are unable to align themselves in the direction of the applied electric field, leading to weak polarization and a low dielectric constant. However, with increasing temperature, the mobility of the charge carriers increases, resulting in enhanced polarization and a higher dielectric constant. The interaction between different valence states of elements found in nanosized ferrites heavily influences the polarization, leading to an increase in dielectric constant as the temperature rises due to a large number of charge carriers releasing and contributing to polarization. The high dielectric constants observed at high frequencies can be attributed to the presence of space charge polarization, which arises due to the inhomogeneous dielectric structure caused by variations in grain size and impurities [201].

$NiFe_2O_4$ has a dielectric structure consisting of conducting grains and grain boundaries. The transfer of electrons between Fe^{2+} and Fe^{3+} ions and holes between Ni^{3+} and Ni^{2+} ions enables electrical conduction and dielectric polarization. However, at higher frequencies, the electron/hole exchange frequency cannot keep up with the applied electric field, leading to lower polarization [202].

1.5.5. Waste water treatment

Industrial wastewater management has become one of the most pressing issues in developed countries in recent years. Textile wastewaters contain a variety of non-biodegradable organic dyes, as well as other pollutants in varying concentrations. Untreated effluents harm not only humans and animals but also plants. RhB is a synthetic, highly poisonous, water-soluble organic dye that is commonly found in the wastewaters and is widely employed as a colorant in various industries. For the treatment of RhB-containing water, various procedures have been used, including ozonation, the electrochemical method, and the Fenton process. In recent years, magnetic NPs have attracted considerable attention due to their special magnetic properties, high adsorption capacities and surface area to volume ratio.

The extensive applications of spinel ferrite NPs in water and wastewater-related treatments have been shown in many studies. The roles of spinel ferrite nanoparticles include their potential use as an adsorbent for pollutants and their ability to catalyze the degradation of organic pollutants under photocatalytic conditions. These applications have been widely studied. $CoFe_2O_4$ is used in wastewater treatment due to its several useful properties. First, it has a high capacity for adsorbing pollutants from water. Second, the material's magnetic properties enable the separation of nanoparticles using an external magnetic field, making it easy to remove them from the water. Finally, $CoFe_2O_4$ has a low energy bandgap, which means it can be used for photocatalytic degradation of RhB when exposed to visible light [203]. Moreover, $CuFe_2O_4$ is also being explored as a potential material for various fields of water purification such as adsorption of toxic metals, degradation of organic dyes and photocatalysis [204]. $CuFe_2O_4$ can be used as cost-effective adsorption for removing MB from water and wastewater when combined with a suitable adsorbent. In addition, $ZnFe_2O_4$ can be utilized as a magnetically recyclable material to remove chemical impurities (such as colors) and biological contaminants from water/industrial wastewater treatment [205]. Kefeni et al. [206] conducted a review on the various applications of spinel ferrite nanoparticles, including their use for disinfecting pathogens, modifying membranes, extracting analytes, and sensing and detecting different types of metal ions in water and wastewater treatment. Similarly, Reddy et al. [1] have reviewed the application of spinel ferrite magnetic as an adsorbent for water purification.

1.5.6. Catalytic applications

Spinel ferrites are commonly used as heterogeneous catalysts due to their ease of recovery from reaction mixtures by filtering or using an external magnetic field, making the process cost-effective and environmentally friendly through their multiple recyclings. To be economically valuable and ecologically friendly, heterogeneous catalytic nanoparticles play a key role in the selective protection of functional groups. The catalytic characteristics of various spinel ferrites (MFe_2O_4, where M is Cu, Ni, Co, or Zn) were evaluated, and the

$CoFe_2O_4$ catalyst showed the most excellent performance with benzaldehyde, achieving 63% conversion and 93% selectivity, while the $CuFe_2O_4$ catalyst demonstrated the best performance with H_2O_2 oxidant, attaining 57.3% conversion and 89.5% selectivity. The catalytic activity of materials is greatly influenced by particle size, surface area, morphology, and chemical composition. The catalytic activity of nanocrystalline spinel ferrites is also influenced by the distribution of cations between tetrahedral (A) and octahedral (B) sites. $CoFe_2O_4$ has been found to exhibit superior catalytic performance compared to other ferrites [207].

1.5.7. Photocatalytic applications

Photocatalysts are important materials that facilitate the use of solar energy in oxidation and reduction reactions, with numerous applications including removing water and air pollution, managing odors, deactivating bacteria, splitting water to generate hydrogen, inactivating cancer cells, and other areas. Currently, photocatalysis is a preferred method for removing dyes, as irradiation of light on a semiconductor can generate electron-hole pairs that can be utilized for oxidation and reduction processes. Dye degradation is caused by the generation of active radicals during the photocatalytic reaction.

There are only a limited number of materials that can perform both photo-oxidation and photo-reduction, meaning they can effectively remove harmful organic compounds while also efficiently absorbing visible light. Ferrites have a wide surface area and many reaction sites due to their small crystallite size, which increases photocatalytic activity. The effectiveness of photocatalysis depends on various factors such as the choice of photocatalyst, size of the nanoparticles, level of crystallinity, accessibility of the active surface to pollutants, and resistance to diffusion of organic pollutants. These parameters can significantly impact the photocatalytic properties of the material. Small particle size and high crystallinity are important factors that enhance the specific surface area and active sites, leading to improved photocatalytic activity. Ferrites are excellent candidates for photocatalysis due to their spinel crystal structure and bandgap that can absorb visible light. They are capable of degrading a wide range of contaminants [208]. Spinel ferrites such as $NiFe^2O^4$, $ZnFe^2O^4$, $CuFe_2O_4$, and $SnFe^2O^4$ have shown light activity, magnetic recyclability, low cost and eco-friendly. These spinel ferrites can be coupled to commonly used photocatalysts to add magnetic properties into it, to help easy separation by an external magnetic field as well as enhance photocatalytic degradation of contaminants and stability. Fe_2O_3 considered as stable semiconductor for photocatalyst reactions due to low band gap (2.3 ev), recyclability earth abundant high harvesting light and excellent stability, and ease of surface modification relative to other spinel ferrites. Heterojunction construction can be an effective strategy to simultaneously utilize high redox potential and broad absorption range which is merely not possible in either bare or doped photocatalysts. Cai et al. [209] showed in photocatalytic mechanism of Zn ferrites based heterojunction, the photon-illuminated electron is migrated to the conduction band reducing Fe^{3+} to Fe^{2+} also generating SO_4^{2-} radical on conduction band. OH at valence band. Removal efficiencies for chemical oxygen demand and organic carbon at 300 min were 50.5% and 78.6%, respectively. (Fig. 14a).

Due to the rapid recombination of charge carrier and small hole dispersion distance, ferrites as the single component doesn't have acceptable performance. Therefore, doping in ferrites suppresses the recombination rate of charges and lower luminescence intensity. Different support materials were utilized to magnify adsorptional ability by increasing surface area and improving thermal and chemical stability. The various support such as SiO_2, g-C_3N_4, carbon nanotubes graphene, and metal organic framework were used (Fig. 14b) [210–213].

1.5.8. Coloring

Ceramic dyes are composed of metal transition oxides and possess exceptional chemical and thermal stability, as well as a high tinting strength when dispersed and fired with glazes or ceramic matrices. They also exhibit a high refractive index, resistance to acid and alkali, and low abrasive strength when dispersed and fired with glazes or ceramic matrices. Each pigment's color is achieved by combining chromophore agents (often transition metals) with an inert oxide matrix.

$CoFe_2O_4$ is a black pigment that is frequently used in the ceramic industry. The performance of the pigment is affected by the coating crystallization, with a higher number of crystals in the glass leading to a brighter color. $ZnFe_2O_4$ NPs have a high covering power and a low cost and are thermally stable, insoluble, and resistant to aggressive media. ZnFe2O4 spinel pigments react with the corrosive environment, producing cationic soaps that enhance the binder's mechanical strength and reduce solubility. During the process of annealing, the color of ZnFe2O4 may be affected by both the particle size and the annealing temperature. This is because annealing can result in a reduction in the total reflecting surface of the powder, which can have an impact on the overall color. The

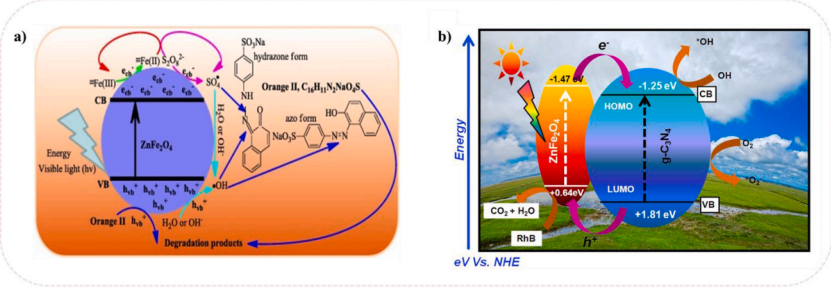

Fig. 14. Photocatalysis mechanism a) $ZnFe_2O_4$/persulfate for orange II degradation [209], b) $ZnFe_2O_4$/g-C_3N_4 hybrid photocatalyst [210].

system undergoes a significant change at high annealing temperatures due to the removal of defects (such as oxygen vacancies), leading to less distorted tetrahedral and octahedral sites and, as a consequence, better-defined color. By selectively choosing cations to occupy specific sites within the spinel lattice (for example, Zn^{2+} in A sites and Fe^{3+} in B sites for $ZnFe_2O_4$), it is possible to modify or create new properties of pigments when dispersed in an organic binder [214].

1.5.9. Corrosion Protection

Metal corrosion is typically caused by an electrochemical reaction in which metal ions dissolve due to the presence of certain factors, such as moisture, oxygen, and chemicals like chloride ions, which can dissolve protective layers of oxides on the metal surface and accelerate the corrosion process. The electrochemical process of metal corrosion can be limited by converting ferrous (Fe^{2+}) ions to ferric (Fe^{3+}) ions, which operate as inorganic corrosion inhibitors. This process can result in the production of a passivation layer that prevents both cathodic and anodic reactions, thus limiting the corrosion of the metallic substrate.

Organic coatings protect against corrosive conditions by acting as a barrier or mechanical protection. Nanocontainers can be incorporated into an organic coating and used to release corrosion inhibitors, thereby protecting the metal substrate from corrosion. Coating with $CoFe_2O_4@SiO_2$ nanoparticles can enhance the corrosion protection performance of coatings by filling and covering free cavities and electrolyte pathways more effectively than using $CoFe_2O_4$ alone. The inclusion of $CoFe_2O_4@SiO_2$ Nano pigment into epoxy coatings improves the coating corrosion resistance noticeably. Moreover, applying a $ZnFe_2O_4$ coating on the surface of particles like diatomite, talc, wollastonite, and kaolin has been found to greatly enhance their corrosion resistance. Surface treatment with low levels of $ZnFe_2O_4$ (16–20 wt %) improves corrosion resistance [215].

1.5.10. Antimicrobial applications

Iron plays a significant role in the development of microbial infections, as many organisms use iron sequestration as a defense mechanism. Microorganisms resistant to Fe^{+2} and Fe^{+3} also display unexpected resistance to several antibiotics. MFe_2O_4 nanoparticles have been shown to possess excellent antibacterial properties against various bacteria and fungi. Escherichia coli has been found to develop resistance to excess iron primarily by changing the way it absorbs iron. CoFe2O4 nanoparticles (NPs) are commonly used for biomedical purposes because of their ability to combat various human infections. Their high surface area-to-volume ratio and nanoscale size make them effective against harmful microorganisms. A nanocomposite called $CoFe_2O_4@SiO_2@Ag$, when combined with Streptomycin, has demonstrated significant antibacterial properties against both Gram-positive and Gram-negative microorganisms. The inclusion of Ag NPs on $CoFe_2O_4@SiO_2$ prevents aggregation and enables easy retrieval from the solution after disinfection through an external magnetic field, owing to the presence of a magnetic core in the composite. $CoFe_2O_4$ attaches to microorganism membranes, lengthening the lag stage of the bacterial growth phase, widening microorganism production time, and enhancing bacterial cell division. The antibacterial activity of $CoFe_2O_4$ nanoparticles is attributed to the generation of superoxide (O^{2-}) and hydrogen peroxide (H_2O_2) that exhibit antibacterial properties. The migration of these effective oxides over the cell membrane of bacteria leads to the antibacterial activity of the ferrite nanoparticles against unicellular fungi.

$ZnFe_2O_4$ nanoparticles have been found to possess effective antibacterial activity against different strains of bacteria, including Lactobacillus, Escherichia coli, Bacillus cereus (which are Gram-positive), and Aeromonas hydrophila and Vibrio harveyi (which are Gram-negative). The antibacterial activity of the nanoparticles was observed to be dependent on their small crystallite size and surface area [216,217].

1.5.11. Biomedical applications

For use in biomedical applications, magnetic nanoparticles need to have high magnetic saturation values and be biocompatible, while also being stable and non-agglomerated when dispersed in water. These nanoparticles can be used within individual cells to facilitate magnetic fluid hyperthermia, drug delivery, and stimulation of metabolic pathways through thermal excitation. $MnFe_2O_4$ nanoparticles have attracted significant interest in the field of biomedicine due to their desirable properties, including simple synthesis, controllable size, high magnetization value, superparamagnetic nature, ability to be monitored by an external magnetic field, and high biocompatibility. The surface modification of $MnFe_2O_4$ NPs by incorporating them into mesoporous SiO_2 nanospheres or coating them with mesoporous SiO_2 can enhance the stability of the nanoparticles in water, improve their biocompatibility, and prevent their agglomeration and degradation.

The physical properties of $CoFe_2O_4$, particularly its great stability, have sparked a lot of interest in possible biomedical applications. $CoFe_2O_4$ has been utilized for medication administration, imaging, and brain tumor therapy in general. At high concentrations of $CoFe_2O_4$ NPs, metal ions are released, and a portion of these ions can enter cells and lead to cytotoxicity. One possible reason for this could be that the inhibition of cell transcription and protein synthesis leads to changes in cellular function. The adverse effects can be eliminated or reduced by applying a biocompatible SiO_2 coating. The coating of $CoFe_2O_4$ NPs caused a decrease in their adhesion as the SiO_2 matrix possessed a negative charge. The NPs exhibited superparamagnetic properties with low MS values, increased compatibility, and became well-suited for medical applications, including drug delivery to cancer cells and the use of a contrast agent for cancer diagnosis in magnetic resonance imaging.

Hyperthermia is a therapeutic procedure used to treat oncological diseases, whereby living tissues containing both healthy and carcinoma cells are exposed to constant overheating (above 43 °C), leading to necrosis. However, hyperthermia induced by magnetic nanoparticles through magnetic induction may provide a promising solution by selectively heating and destroying tumor tissue while minimizing damage to healthy tissue.

Magnetic hyperthermia is a recently developed supplementary treatment for malignant tumors that involves the use of appropriate magnetic nanoparticles in a magnetic field, generating heat that aids in the elimination of damaged tissues at a temperature ranging

between 41 and 46 °C. Under a time-varying magnetic field, ferromagnetic materials have hysteretic characteristics, which cause magnetically induced heating. Furthermore, magnetic nanoparticles have low toxicity, are biocompatible, and are well-tolerated by living organisms, enabling an easy and rapid evaluation of their specific absorption rates. According to some studies, magnetophoresis, which is created by a magnetic field gradient acting on the magnetically induced magnetic moment of a particle, has been proposed as an effective method for delivering ferrimagnetic nanoparticles to a tumor site. Magnetophoresis is also utilized to separate magnetic NPs hanging in fluids in a variety of commercial and industrial procedures. The fundamental challenge of hyperthermia, on the other hand, is to minimize harm to neighboring normal tissues. In this case, it is crucial that the nanoparticles are specifically targeted and localized at the tumor site rather than in the surrounding area [218,219].

2. Future scope and challenges

Nanoscale spinel ferrites have become a topic of significant interest in the past few decades, owing to their distinctive characteristics such as stability in chemical and thermal environments, significant coercivity, elevated anisotropy constant and Curie temperature, moderate saturation magnetization, high electrical resistance, and minimal loss of eddy current. The appropriate features of magnetic spinel ferrites together with the typical modifications and functionalizations generate new prospects for its future use in biomedicine, catalyst, water treatment, and energy fields. It is clear that the upcoming trend in magnetic spinel ferrites applications will focus on controlling the required magnetic properties through modification of the synthetic methods, which will result in fine-tuning of the particle size, shape, and crystallinity. The physical and chemical properties of spinel ferrites not only depend on the synthesis methods and modification but also doping is another effective method in preparation of nonaggregated and monodisperse nanosized spinel ferrites.

One of application of magnetic spinel ferrites is as efficient magnetic materials in magnetic hyperthermia. Although many studies have reported the use of spinel ferrite-based materials for the hyperthermia, it is still in its infancy stage, and some challenges such as tuning size, shape and magnetic properties of nanoparticles need further study. In addition, efficient methods for modifying the surface of spinel ferrites should be further explored in the future, one of the most important issues to obtain magnetic ferrite nanoparticles whose performance is expected for biomedical applications.

Although the applications of magnetic spinel ferrites have been extended for waste water treatment, some challenges need to be addressed in future studies to develop photocatalytic properties of spinel ferrite nanoparticles for degradation of organic pollutants.

3. Conclusion

Recently MFe_2O_4 materials have received a lot of attention due to its unique features, including stability under mechanical, chemical, and thermal conditions, high coercivity, elevated anisotropy constant and Curie temperature, high electrical resistance, moderate saturation magnetization, and minimal eddy current loss. Among all the reviewed synthesis strategies, the usefulness of MFe_2O_4 in many applications depends largely on the synthesis processes; efficient synthesis processes yield MFe_2O_4 that can function better and endure the conditions under which they are synthesized. Nevertheless, the cost-effective synthesis of large amounts of MFe_2O_4 with monodisperse size and shape for a biomedical purposes, however, needs more study and it is important to take into account and thoroughly examine the toxicity of specific MFe_2O_4 NPs.

Author contribution statement

All authors listed have significantly contributed to the development and the writing of this article.

Data availability statement

No data was used for the research described in the article.

Declaration of competing interest

The authors declare that they have no known competing financial interests or personal relationships that could have appeared to influence the work reported in this paper.

References

[1] D.H.K. Reddy, Y.-S. Yun, Spinel ferrite magnetic adsorbents: alternative future materials for water purification? Coord. Chem. Rev. 315 (2016) 90–111.
[2] K.K. Kefeni, B.B. Mamba, Photocatalytic application of spinel ferrite nanoparticles and nanocomposites in wastewater treatment, Sustainable materials and technologies 23 (2020), e00140.
[3] S. Mokhosi, W. Mdlalose, S. Mngadi, M. Singh, T. Moyo, Assessing the structural, morphological and magnetic properties of polymer-coated magnesium-doped cobalt ferrite (CoFe2O4) nanoparticles for biomedical application, in: Journal of Physics: Conference Series, IOP Publishing, 2019.
[4] S. Chakrabarty, M. Pal, A. Dutta, Yttrium doped cobalt ferrite nanoparticles: study of dielectric relaxation and charge carrier dynamics, Ceram. Int. 44 (12) (2018) 14652–14659.
[5] G. Asab, E.A. Zereffa, T. Abdo Seghne, Synthesis of silica-coated fe3o4 nanoparticles by microemulsion method: characterization and evaluation of antimicrobial activity, International journal of biomaterials (2020) 2020.
[6] M. Anand, Hysteresis in a linear chain of magnetic nanoparticles, J. Appl. Phys. 128 (2) (2020), 023903.

[7] T. Sodaee, A. Ghasemi, R.S. Razavi, Cation distribution and microwave absorptive behavior of gadolinium substituted cobalt ferrite ceramics, J. Alloys Compd. 706 (2017) 133–146.
[8] H. Kardile, S.B. Somvanshi, A.R. Chavan, A. Pandit, K. Jadhav, Effect of Cd2+ doping on structural, morphological, optical, magnetic and wettability properties of nickel ferrite thin films, Optik 207 (2020), 164462.
[9] N. Amri, J. Massoudi, K. Nouri, M. Triki, E. Dhahri, L. Bessais, Influence of neodymium substitution on structural, magnetic and spectroscopic properties of Ni–Zn–Al nano-ferrites, RSC Adv. 11 (22) (2021) 13256–13268.
[10] V. Anjana, S. John, P. Prakash, A.M. Nair, A.R. Nair, S. Sambhudevan, B. Shankar, Magnetic properties of copper doped nickel ferrite nanoparticles synthesized by Co precipitation method, in: IOP Conference Series: Materials Science and Engineering, IOP Publishing, 2018.
[11] M. Ahmad, M.A. Khan, A. Mahmood, S.-S. Liu, A.H. Chughtai, W.-C. Cheong, B. Akram, G. Nasar, Role of ytterbium on structural and magnetic properties of NiCr0. 1Fe1. 9O4 co-precipitated ferrites, Ceram. Int. 44 (5) (2018) 5433–5439.
[12] R. Sharma, P. Thakur, P. Sharma, V. Sharma, Mn 2+ doped Mg–Zn ferrite nanoparticles for microwave device applications, IEEE Electron. Device Lett. 39 (6) (2018) 901–904.
[13] M. Satheeshkumar, E.R. Kumar, C. Srinivas, N. Suriyanarayanan, M. Deepty, C. Prajapat, T.C. Rao, D. Sastry, Study of structural, morphological and magnetic properties of Ag substituted cobalt ferrite nanoparticles prepared by honey assisted combustion method and evaluation of their antibacterial activity, J. Magn. Magn Mater. 469 (2019) 691–697.
[14] A.H. Oh, H.-Y. Park, Y.-G. Jung, S.-C. Choi, G.S. An, Synthesis of Fe3O4 nanoparticles of various size via the polyol method, Ceram. Int. 46 (8) (2020) 10723–10728.
[15] H.M.K. Tedjieukeng, P.K. Tsobnang, R.L. Fomekong, E.P. Etape, P.A. Joy, A. Delcorte, J.N. Lambi, Structural characterization and magnetic properties of undoped and copper-doped cobalt ferrite nanoparticles prepared by the octanoate coprecipitation route at very low dopant concentrations, RSC Adv. 8 (67) (2018) 38621–38630.
[16] P. Hu, T. Chang, W.-J. Chen, J. Deng, S.-L. Li, Y.-G. Zuo, L. Kang, F. Yang, M. Hostetter, A.A. Volinsky, Temperature effects on magnetic properties of Fe3O4 nanoparticles synthesized by the sol-gel explosion-assisted method, J. Alloys Compd. 773 (2019) 605–611.
[17] M.P. Ghosh, S. Datta, R. Sharma, K. Tanbir, M. Kar, S. Mukherjee, Copper doped nickel ferrite nanoparticles: jahn-Teller distortion and its effect on microstructural, magnetic and electronic properties, Mater. Sci. Eng., B 263 (2021), 114864.
[18] M. Rashad, D. Rayan, A. Turky, M. Hessien, Effect of Co2+ and Y3+ ions insertion on the microstructure development and magnetic properties of Ni0. 5Zn0. 5Fe2O4 powders synthesized using co-precipitation method, J. Magn. Magn Mater. 374 (2015) 359–366.
[19] H. Mund, B. Ahuja, Structural and magnetic properties of Mg doped cobalt ferrite nano particles prepared by sol-gel method, Mater. Res. Bull. 85 (2017) 228–233.
[20] H. Moradmard, S.F. Shayesteh, P. Tohidi, Z. Abbas, M. Khaleghi, Structural, magnetic and dielectric properties of magnesium doped nickel ferrite nanoparticles, J. Alloys Compd. 650 (2015) 116–122.
[21] M. Hashim, A. Ahmed, S.A. Ali, S.E. Shirsath, M.M. Ismail, R. Kumar, S. Kumar, S.S. Meena, D. Ravinder, Structural, optical, elastic and magnetic properties of Ce and Dy doped cobalt ferrites, J. Alloys Compd. 834 (2020), 155089.
[22] O.K. Mmelesi, N. Masunga, A. Kuvarega, T.T. Nkambule, B.B. Mamba, K.K. Kefeni, Cobalt ferrite nanoparticles and nanocomposites: photocatalytic, antimicrobial activity and toxicity in water treatment, Mater. Sci. Semicond. Process. 123 (2021), 105523.
[23] G. Rana, P. Dhiman, A. Kumar, D.-V.N. Vo, G. Sharma, S. Sharma, M. Naushad, Recent advances on nickel nano-ferrite: a review on processing techniques, properties and diverse applications, Chem. Eng. Res. Des. 175 (2021) 182–208.
[24] J. Xu, H. Yang, W. Fu, K. Du, Y. Sui, J. Chen, Y. Zeng, M. Li, G. Zou, Preparation and magnetic properties of magnetite nanoparticles by sol–gel method, J. Magn. Magn Mater. 309 (2) (2007) 307–311.
[25] V. Vinayak, P.P. Khirade, S.D. Birajdar, P. Gaikwad, N. Shinde, K. Jadhav, Low temperature synthesis of magnesium doped cobalt ferrite nanoparticles and their structural properties, International Advanced Research Journal in Science, Engineering and Technology 2 (3) (2015).
[26] R. Kumar, H. Kumar, R.R. Singh, P. Barman, Variation in magnetic and structural properties of Co-doped Ni–Zn ferrite nanoparticles: a different aspect, J. Sol. Gel Sci. Technol. 78 (3) (2016) 566–575.
[27] B.I. Kharisov, H.R. Dias, O.V. Kharissova, Mini-review: ferrite nanoparticles in the catalysis, Arab. J. Chem. 12 (7) (2019) 1234–1246.
[28] R.G. Andrade, S.R. Veloso, E. Castanheira, Shape anisotropic iron oxide-based magnetic nanoparticles: synthesis and biomedical applications, Int. J. Mol. Sci. 21 (7) (2020) 2455.
[29] A.B. Mapossa, W. Mhike, J.L. Adalima, S. Tichapondwa, Removal of organic dyes from water and wastewater using magnetic ferrite-based titanium oxide and zinc oxide nanocomposites: a review, Catalysts 11 (12) (2021) 1543.
[30] A. Soudi, H. Hajjaoui, R. Elmoubarki, M. Abderrouri, S. Qourazl, N. Barka, Spinel ferrites nanoparticles: synthesis methods and application in heterogeneous Fenton oxidation of organic pollutants–a review, Applied Surface Science Advances 6 (2021), 100145.
[31] S.B. Narang, K. Pubby, Nickel spinel ferrites: a review, J. Magn. Magn Mater. 519 (2021), 167163.
[32] Z. Li, J. Dai, C. Cheng, Z. Suo, Synthesis and magnetic properties of chromium doped cobalt ferrite nanotubes, Mater. Res. Express 7 (8) (2020), 086102.
[33] B. Patil, R. Kokate, Synthesis and design of magnetic parameters by Ti doping in cobalt ferrite nanoparticles for nanoelectronics applications, Procedia Manuf. 20 (2018) 147–153.
[34] O.K. Mmelesi, N. Masunga, A. Kuvarega, T.T. Nkambule, B.B. Mamba, K.K. Kefeni, Cobalt ferrite nanoparticles and nanocomposites: photocatalytic, antimicrobial activity and toxicity in water treatment, Mater. Sci. Semicond. Process. (2020), 105523.
[35] M. Shobana, W. Nam, H. Choe, Yttrium-doped cobalt nanoferrites prepared by sol–gel combustion method and its characterization, J. Nanosci. Nanotechnol. 13 (5) (2013) 3535–3538.
[36] D. Cao, L. Pan, J. Li, X. Cheng, Z. Zhao, J. Xu, Q. Li, X. Wang, S. Li, J. Wang, Investigation on the structures and magnetic properties of carbon or nitrogen doped cobalt ferrite nanoparticles, Sci. Rep. 8 (1) (2018) 1–9.
[37] S. ullah Rather, O. Lemine, Effect of Al doping in zinc ferrite nanoparticles and their structural and magnetic properties, J. Alloys Compd. 812 (2020), 152058.
[38] R. Haghniaz, A. Rabbani, F. Vajhadin, T. Khan, R. Kousar, A.R. Khan, H. Montazerian, J. Iqbal, A. Libanori, H.-J. Kim, Anti-bacterial and wound healing-promoting effects of zinc ferrite nanoparticles, J. Nanobiotechnol. 19 (1) (2021) 1–15.
[39] A. Safari, K. Gheisari, M. Farbod, Structural, microstructural, magnetic and dielectric properties of Ni-Zn ferrite powders synthesized by plasma arc discharge process followed by post-annealing, J. Magn. Magn Mater. 488 (2019), 165369.
[40] R.M. Borade, S.B. Somvanshi, S.B. Kale, R.P. Pawar, K. Jadhav, Spinel zinc ferrite nanoparticles: an active nanocatalyst for microwave irradiated solvent free synthesis of chalcones, Mater. Res. Express 7 (1) (2020), 016116.
[41] J. Isasi, P. Arévalo, E. Martin, F. Martín-Hernández, Preparation and study of silica and APTES–silica-modified NiFe 2 O 4 nanocomposites for removal of Cu 2 + and Zn 2+ ions from aqueous solutions, J. Sol. Gel Sci. Technol. 91 (3) (2019) 596–610.
[42] G.N. Rajivgandhi, G. Ramachandran, C.C. Kanisha, N.S. Alharbi, S. Kadaikunnan, J.M. Khaled, K.F. Alanzi, W.-J. Li, Effect of Ti and Cu doping on the structural, optical, morphological and anti-bacterial properties of nickel ferrite nanoparticles, Results Phys. 23 (2021), 104065.
[43] J. Hwang, M. Choi, H.-S. Shin, B.-K. Ju, M. Chun, Structural and magnetic properties of NiZn ferrite nanoparticles synthesized by a thermal decomposition method, Appl. Sci. 10 (18) (2020) 6279.
[44] W.A. Khoso, N. Haleem, M.A. Baig, Y. Jamal, Synthesis, characterization and heavy metal removal efficiency of nickel ferrite nanoparticles (NFN's), Sci. Rep. 11 (1) (2021) 1–10.
[45] H. Abdolmohammad-Zadeh, A. Salimi, Preconcentration of Pb (II) by using Mg (II)-doped NiFe 2 O 4 nanoparticles as a magnetic solid phase extraction agent, Microchim. Acta 185 (7) (2018) 1–8.
[46] M.A. Yousuf, M.M. Baig, N.F. Al-Khalli, M.A. Khan, M.F.A. Aboud, I. Shakir, M.F. Warsi, The impact of yttrium cations (Y3+) on structural, spectral and dielectric properties of spinel manganese ferrite nanoparticles, Ceram. Int. 45 (8) (2019) 10936–10942.

[47] H.L. Andersen, M. Saura-Múzquiz, C. Granados-Miralles, E. Canévet, N. Lock, M. Christensen, Crystalline and magnetic structure–property relationship in spinel ferrite nanoparticles, Nanoscale 10 (31) (2018) 14902–14914.
[48] S. Tsopoe, J. Borah, C. Borgohain, An investigation of mixed spinel ferrite Co0. 5Zn0. 5Fe2O4 nanoparticles for effective magnetic fluid hyperthermia applications, Mater. Today: Proc. 68 (2022) 163–166.
[49] M. Ansari, A. Bigham, H.A. Ahangar, Super-paramagnetic nanostructured CuZnMg mixed spinel ferrite for bone tissue regeneration, Mater. Sci. Eng. C 105 (2019), 110084.
[50] H. Zaki, S. Al-Heniti, T. Elmosalami, Structural, magnetic and dielectric studies of copper substituted nano-crystalline spinel magnesium zinc ferrite, J. Alloys Compd. 633 (2015) 104–114.
[51] R. Lamouri, O. Mounkachi, E. Salmani, M. Hamedoun, A. Benyoussef, H. Ez-Zahraouy, Size effect on the magnetic properties of CoFe2O4 nanoparticles: a Monte Carlo study, Ceram. Int. 46 (6) (2020) 8092–8096.
[52] W. Mazgaj, M. Sierzega, Z. Szular, Approximation of hysteresis changes in electrical steel sheets, Energies 14 (14) (2021) 4110.
[53] P. Prudnikov, V. Prudnikov, I. Saifutdinov, Simulation of hysteresis phenomena in multilayer magnetic nanostructures, in: Journal of Physics: Conference Series, IOP Publishing, 2021.
[54] B. Vara Prasad, K. Ramesh, A. Srinivas, Structural and magnetic studies of nano-crystalline ferrites MFe2O4 (M= Zn, Ni, Cu, and Co) synthesized via citrate gel autocombustion method, J. Supercond. Nov. Magnetism 30 (12) (2017) 3523–3535.
[55] W. Mohamed, M. Alzaid, M. Sm Abdelbaky, Z. Amghouz, S. García-Granda, A.M. Abu-Dief, Impact of Co2+ substitution on microstructure and magnetic properties of CoxZn1-xFe2O4 nanoparticles, Nanomaterials 9 (11) (2019) 1602.
[56] S. Mazen, H. Elsayed, N. Abu-Elsaad, Effect of divalent metal ions substitution on structural and magnetic properties of Li0. 25Mn0. 5-xMxFe2. 25O4 (M= Co2+, Ni2+, Cu2+) spinel ferrites, Mater. Chem. Phys. 256 (2020), 123676.
[57] B. Purnama, A.T. Wijayanta, Effect of calcination temperature on structural and magnetic properties in cobalt ferrite nano particles, J. King Saud Univ. Sci. 31 (4) (2019) 956–960.
[58] S. Liu, B. Yu, S. Wang, Y. Shen, H. Cong, Preparation, surface functionalization and application of Fe3O4 magnetic nanoparticles, Adv. Colloid Interface Sci. 281 (2020), 102165.
[59] A. Allafchian, S.S. Hosseini, Antibacterial magnetic nanoparticles for therapeutics: a review, IET Nanobiotechnol. 13 (8) (2019) 786–799.
[60] P. Kumar, H. Khanduri, S. Pathak, A. Singh, G. Basheed, R. Pant, Temperature selectivity for single phase hydrothermal synthesis of PEG-400 coated magnetite nanoparticles, Dalton Trans. 49 (25) (2020) 8672–8683.
[61] S. Kanagesan, M. Hashim, S. Ab Aziz, I. Ismail, S. Tamilselvan, N.B. Alitheen, M.K. Swamy, B. Purna Chandra Rao, Evaluation of antioxidant and cytotoxicity activities of copper ferrite (CuFe2O4) and zinc ferrite (ZnFe2O4) nanoparticles synthesized by sol-gel self-combustion method, Appl. Sci. 6 (9) (2016) 184.
[62] M. Vishwas, K.V. Babu, K.A. Gowda, S.B. Gandla, Synthesis, characterization and photo-catalytic activity of magnetic CoFe2O4 nanoparticles prepared by temperature controlled co-precipitation method, Mater. Today: Proc. (2022).
[63] Z. Mahhouti, H. El Moussaoui, T. Mahfoud, M. Hamedoun, M. El Marssi, A. Lahmar, A. El Kenz, A. Benyoussef, Chemical synthesis and magnetic properties of monodisperse cobalt ferrite nanoparticles, J. Mater. Sci. Mater. Electron. 30 (16) (2019) 14913–14922.
[64] A.A. Rodríguez-Rodríguez, M.B. Moreno-Trejo, M.J. Meléndez-Zaragoza, V. Collins-Martínez, A. López-Ortiz, E. Martínez-Guerra, M. Sánchez-Domínguez, Spinel-type ferrite nanoparticles: synthesis by the oil-in-water microemulsion reaction method and photocatalytic water-splitting evaluation, Int. J. Hydrogen Energy 44 (24) (2019) 12421–12429.
[65] R. Melo, P. Banerjee, A. Franco, Hydrothermal synthesis of nickel doped cobalt ferrite nanoparticles: optical and magnetic properties, J. Mater. Sci. Mater. Electron. 29 (17) (2018) 14657–14667.
[66] R.S. Yadav, I. Kuřitka, J. Vilcakova, J. Havlica, L. Kalina, P. Urbánek, M. Machovsky, D. Skoda, M. Masař, M. Holek, Sonochemical synthesis of Gd3+ doped CoFe2O4 spinel ferrite nanoparticles and its physical properties, Ultrason. Sonochem. 40 (2018) 773–783.
[67] A. Shukla, A.K. Bhardwaj, S. Singh, K. Uttam, N. Gautam, A. Himanshu, J. Shah, R. Kotnala, R. Gopal, Microwave assisted scalable synthesis of titanium ferrite nanomaterials, J. Appl. Phys. 123 (16) (2018), 161411.
[68] M.R. Zamani Kouhpanji, B.J. Stadler, A guideline for effectively synthesizing and characterizing magnetic nanoparticles for advancing nanobiotechnology: a review, Sensors 20 (9) (2020) 2554.
[69] M.S. Samadi, H. Shokrollahi, A. Zamanian, The magnetic-field-assisted synthesis of the Co-ferrite nanoparticles via reverse co-precipitation and their magnetic and structural properties, Mater. Chem. Phys. 215 (2018) 355–359.
[70] P. Thakur, D. Chahar, S. Taneja, N. Bhalla, A. Thakur, A review on MnZn ferrites: synthesis, characterization and applications, Ceram. Int. 46 (10) (2020) 15740–15763.
[71] C. Sedrati, S. Alleg, H. Boussafel, A. Bendali Hacine, Structure and magnetic properties of nickel ferrites synthesized by a facile co-precipitation method: effect of the Fe/Ni ratio, J. Mater. Sci. Mater. Electron. 32 (19) (2021) 24548–24559.
[72] Y. Peng, C. Xia, M. Cui, Z. Yao, X. Yi, Effect of reaction condition on microstructure and properties of (NiCuZn) Fe2O4 nanoparticles synthesized via co-precipitation with ultrasonic irradiation, Ultrason. Sonochem. 71 (2021), 105369.
[73] C.R. Kalaiselvan, S.S. Laha, S.B. Somvanshi, T.A. Tabish, N.D. Thorat, N.K. Sahu, Manganese ferrite (MnFe2O4) nanostructures for cancer theranostics, Coord. Chem. Rev. 473 (2022), 214809.
[74] T.N. Pham, T.Q. Huy, A.-T. Le, Spinel ferrite (AFe 2 O 4)-based heterostructured designs for lithium-ion battery, environmental monitoring, and biomedical applications, RSC Adv. 10 (52) (2020) 31622–31661.
[75] M. Sanna Angotzi, V. Mameli, C. Cara, V. Grillo, S. Enzo, A. Musinu, C. Cannas, Defect-assisted synthesis of magneto-plasmonic silver-spinel ferrite heterostructures in a flower-like architecture, Sci. Rep. 10 (1) (2020) 1–13.
[76] H. Zhang, J. Hu, M. Li, Z. Li, Y. Yuan, X. Yang, L. Guo, Highly efficient toluene gas sensor based on spinel structured hollow urchin-like core-shell ZnFe2O4 spheres, Sensor. Actuator. B Chem. 349 (2021), 130734.
[77] Z. Rouhani, J. Karimi-Sabet, M. Mehdipourghazi, A. Hadi, A. Dastbaz, Response surface optimization of hydrothermal synthesis of Bismuth ferrite nanoparticles under supercritical water conditions: application for photocatalytic degradation of Tetracycline, Environ. Nanotechnol. Monit. Manag. 11 (2019), 100198.
[78] S. Fayazzadeh, M. Khodaei, M. Arani, S. Mahdavi, T. Nizamov, A. Majouga, Magnetic properties and magnetic hyperthermia of cobalt ferrite nanoparticles synthesized by hydrothermal method, J. Supercond. Nov. Magnetism 33 (7) (2020) 2227–2233.
[79] K. Rajashekhar, J.L. Naik, M. Prasad, C. Venkateshwarlu, K.M. Kumar, Brief Review on the Effect of Synthesis Method and Doping on the Structure and Magnetic Properties of Zinc Ferrites, 2020.
[80] F.d.A. La Porta, C.A. Taft, Emerging Research in Science and Engineering Based on Advanced Experimental and Computational Strategies, 2020.
[81] E. Meydan, S. Demirci, N. Aktas, N. Sahiner, O.F. Ozturk, Catalytic performance of boron-containing magnetic metal nanoparticles in methylene blue degradation reaction and mixture with other pollutants, Inorg. Chem. Commun. 126 (2021), 108474.
[82] F. Sharifianjazi, M. Moradi, N. Parvin, A. Nemati, A.J. Rad, N. Sheysi, A. Abouchenari, A. Mohammadi, S. Karbasi, Z. Ahmadi, Magnetic CoFe2O4 nanoparticles doped with metal ions: a review, Ceram. Int. 46 (11) (2020) 18391–18412.
[83] S. Gul, S.B. Khan, I.U. Rehman, M.A. Khan, M. Khan, A comprehensive review of magnetic nanomaterials modern day theranostics, Frontiers in Materials 6 (2019) 179.
[84] R. Chandunika, R. Vijayaraghavan, N.K. Sahu, Magnetic hyperthermia application of MnFe2O4 nanostructures processed through solvents with the varying boiling point, Mater. Res. Express 7 (6) (2020), 064002.
[85] P.B. Balakrishnan, N. Silvestri, T. Fernandez-Cabada, F. Marinaro, S. Fernandes, S. Fiorito, M. Miscuglio, D. Serantes, S. Ruta, K. Livesey, Exploiting unique alignment of cobalt ferrite nanoparticles, mild hyperthermia, and controlled intrinsic cobalt toxicity for cancer therapy, Adv. Mater. 32 (45) (2020), 2003712.
[86] K.K. Kefeni, T.A. Msagati, T.T. Nkambule, B.B. Mamba, Spinel ferrite nanoparticles and nanocomposites for biomedical applications and their toxicity, Mater. Sci. Eng. C 107 (2020), 110314.

[87] N. Sanpo, J. Tharajak, Y. Li, C.C. Berndt, C. Wen, J. Wang, Biocompatibility of transition metal-substituted cobalt ferrite nanoparticles, J. Nanoparticle Res. 16 (7) (2014) 1–13.
[88] S.B. Somvanshi, M.V. Khedkar, P.B. Kharat, K. Jadhav, Influential diamagnetic magnesium (Mg2+) ion substitution in nano-spinel zinc ferrite (ZnFe2O4): thermal, structural, spectral, optical and physisorption analysis, Ceram. Int. 46 (7) (2020) 8640–8650.
[89] T. Tatarchuk, M. Bououdina, J. Judith Vijaya, L. John Kennedy, Spinel ferrite nanoparticles: synthesis, crystal structure, properties, and perspective applications, in: Nanophysics, Nanomaterials, Interface Studies, and Applications: Selected Proceedings of the 4th International Conference Nanotechnology and Nanomaterials (NANO2016), August 24-27, 2016, Springer, Lviv, Ukraine, 2017.
[90] A. Varma, A.S. Mukasyan, A.S. Rogachev, K.V. Manukyan, Solution combustion synthesis of nanoscale materials, Chem. Rev. 116 (23) (2016) 14493–14586.
[91] A. Sutka, G. Mezinskis, Sol-gel auto-combustion synthesis of spinel-type ferrite nanomaterials, Front. Mater. Sci. 6 (2) (2012) 128–141.
[92] A.S. Mukasyan, P. Epstein, P. Dinka, Solution combustion synthesis of nanomaterials, Proc. Combust. Inst. 31 (2) (2007) 1789–1795.
[93] R.R. Bhosale, A. Kumar, F. AlMomani, I. Alxneit, Propylene oxide assisted sol–gel synthesis of zinc ferrite nanoparticles for solar fuel production, Ceram. Int. 42 (2) (2016) 2431–2438.
[94] D. Ramimoghadam, S. Bagheri, S.B. Abd Hamid, Progress in electrochemical synthesis of magnetic iron oxide nanoparticles, J. Magn. Magn Mater. 368 (2014) 207–229.
[95] J.G. Ovejero, A. Mayoral, M. Cañete, M. García, A. Hernando, P. Herrasti, Electrochemical synthesis and magnetic properties of MFe2O4 (M= Fe, Mn, Co, Ni) nanoparticles for potential biomedical applications, J. Nanosci. Nanotechnol. 19 (4) (2019) 2008–2015.
[96] M. Rivero, A. del Campo, Á. Mayoral, E. Mazario, J. Sánchez-Marcos, A. Muñoz-Bonilla, Synthesis and structural characterization of Zn x Fe 3− x O 4 ferrite nanoparticles obtained by an electrochemical method, RSC Adv. 6 (46) (2016) 40067–40076.
[97] K. Wu, D. Liu, W. Lu, K. Zhang, One-pot sonochemical synthesis of magnetite@ reduced graphene oxide nanocomposite for high performance Li ion storage, Ultrason. Sonochem. 45 (2018) 167–172.
[98] M. Almessiere, Y. Slimani, S. Guner, M. Sertkol, A.D. Korkmaz, S.E. Shirsath, A. Baykal, Sonochemical synthesis and physical properties of Co0. 3Ni0. 5Mn0. 2EuxFe2− xO4 nano-spinel ferrites, Ultrason. Sonochem. 58 (2019), 104654.
[99] Y. Slimani, M. Almessiere, A.D. Korkmaz, S. Guner, H. Güngüneş, M. Sertkol, A. Manikandan, A. Yildiz, S. Akhtar, S.E. Shirsath, Ni0. 4Cu0. 2Zn0. 4TbxFe2-xO4 nanospinel ferrites: ultrasonic synthesis and physical properties, Ultrason. Sonochem. 59 (2019), 104757.
[100] A.M. Ilosvai, D. Dojcsak, C. Váradi, M. Nagy, F. Kristály, B. Fiser, B. Viskolcz, L. Vanyorek, Sonochemical combined synthesis of nickel ferrite and cobalt ferrite magnetic nanoparticles and their application in glycan analysis, Int. J. Mol. Sci. 23 (9) (2022) 5081.
[101] J.H. Bang, K.S. Suslick, Applications of ultrasound to the synthesis of nanostructured materials, Adv. Mater. 22 (10) (2010) 1039–1059.
[102] J.s.A. Fuentes-García, A. Carvalho Alavarse, A.C. Moreno Maldonado, A. Toro-Córdova, M.R. Ibarra, G.F.n. Goya, Simple sonochemical method to optimize the heating efficiency of magnetic nanoparticles for magnetic fluid hyperthermia, ACS Omega 5 (41) (2020) 26357–26364.
[103] R.S. Yadav, I. Kuřitka, J. Vilcakova, T. Jamatia, M. Machovsky, D. Skoda, P. Urbánek, M. Masař, M. Urbánek, L. Kalina, Impact of sonochemical synthesis condition on the structural and physical properties of MnFe2O4 spinel ferrite nanoparticles, Ultrason. Sonochem. 61 (2020), 104839.
[104] S.R. Yousefi, O. Amiri, M. Salavati-Niasari, Control sonochemical parameter to prepare pure Zn0. 35Fe2. 65O4 nanostructures and study their photocatalytic activity, Ultrason. Sonochem. 58 (2019), 104619.
[105] M. Sertkol, Y. Slimani, M. Almessiere, H. Sozeri, R. Jermy, A. Manikandan, S. Shirsath, A. Ui-Hamid, A. Baykal, Sonochemical synthesis of Mn0. 5Zn0. 5ErxDyxFe2-2xO4 (x≤ 0.1) spinel nanoferrites: magnetic and textural investigation, J. Mol. Struct. 1258 (2022), 132680.
[106] M. Tsuji, Microwave-assisted synthesis of metallic nanomaterials in liquid phase, ChemistrySelect 2 (2) (2017) 805–819.
[107] Y.-J. Zhu, F. Chen, Microwave-assisted preparation of inorganic nanostructures in liquid phase, Chem. Rev. 114 (12) (2014) 6462–6555.
[108] M.A. Maksoud, N. Sami, H. Hassan, M. Bekhit, A. Ashour, Novel adsorbent based on carbon-modified zirconia/spinel ferrite nanostructures: evaluation for the removal of cobalt and europium radionuclides from aqueous solutions, J. Colloid Interface Sci. (2021).
[109] C.M. Magdalane, G.M.A. Priyadharsini, K. Kaviyarasu, A.I. Jothi, G.G. Simiyon, Synthesis and characterization of TiO2 doped cobalt ferrite nanoparticles via microwave method: investigation of photocatalytic performance of Congo red degradation dye, Surface. Interfac. 25 (2021), 101296.
[110] M.M. Naik, H. Naik, N. Kottam, M. Vinuth, G. Nagaraju, M. Prabhakara, Multifunctional properties of microwave-assisted bioengineered nickel doped cobalt ferrite nanoparticles, J. Sol. Gel Sci. Technol. 91 (3) (2019) 578–595.
[111] S. Kalia, A. Kumar, N. Munjal, N. Prasad, Synthesis of ferrites using various parts of plants: a mini review, in: Journal of Physics: Conference Series, IOP Publishing, 2021.
[112] P. Thakur, S. Taneja, D. Chahar, B. Ravelo, A. Thakur, Recent advances on synthesis, characterization and high frequency applications of Ni-Zn ferrite nanoparticles, J. Magn. Magn Mater. 530 (2021), 167925.
[113] Y.P. Yew, K. Shameli, M. Miyake, N.B.B.A. Khairudin, S.E.B. Mohamad, T. Naiki, K.X. Lee, Green biosynthesis of superparamagnetic magnetite Fe3O4 nanoparticles and biomedical applications in targeted anticancer drug delivery system: a review, Arab. J. Chem. 13 (1) (2020) 2287–2308.
[114] T.A. Wani, G. Suresh, Plant-mediated green synthesis of magnetic spinel ferrite nanoparticles: a sustainable trend in nanotechnology, Advanced Sustainable Systems (2022), 2200035.
[115] A.A. Bharde, R.Y. Parikh, M. Baidakova, S. Jouen, B. Hannoyer, T. Enoki, B. Prasad, Y.S. Shouche, S. Ogale, M. Sastry, Bacteria-mediated precursor-dependent biosynthesis of superparamagnetic iron oxide and iron sulfide nanoparticles, Langmuir 24 (11) (2008) 5787–5794.
[116] R. Chutia, B. Chetia, Biogenic CuFe 2 O 4 magnetic nanoparticles as a green, reusable and excellent nanocatalyst for acetylation reactions under solvent-free conditions, New J. Chem. 42 (18) (2018) 15200–15206.
[117] G. Karunakaran, M. Jagathambal, N. Van Minh, E. Kolesnikov, D. Kuznetsov, Green synthesis of NiFe2O4 spinel-structured nanoparticles using Hydrangea paniculata flower extract with excellent magnetic property, JOM 70 (7) (2018) 1337–1343.
[118] T. Perez-Gonzalez, C. Jimenez-Lopez, A.L. Neal, F. Rull-Perez, A. Rodriguez-Navarro, A. Fernandez-Vivas, E. Iañez-Pareja, Magnetite biomineralization induced by Shewanella oneidensis, Geochem. Cosmochim. Acta 74 (3) (2010) 967–979.
[119] Y. Amemiya, A. Arakaki, S.S. Staniland, T. Tanaka, T. Matsunaga, Controlled formation of magnetite crystal by partial oxidation of ferrous hydroxide in the presence of recombinant magnetotactic bacterial protein Mms6, Biomaterials 28 (35) (2007) 5381–5389.
[120] W. Zhou, W. He, S. Zhong, Y. Wang, H. Zhao, Z. Li, S. Yan, Biosynthesis and magnetic properties of mesoporous Fe3O4 composites, J. Magn. Magn Mater. 321 (8) (2009) 1025–1028.
[121] W. Zhou, W. He, X. Zhang, S. Yan, X. Sun, X. Tian, X. Han, Biosynthesis of iron phosphate nanopowders, Powder Technol. 194 (1–2) (2009) 106–108.
[122] S. Bose, M.F. Hochella Jr., Y.A. Gorby, D.W. Kennedy, D.E. McCready, A.S. Madden, B.H. Lower, Bioreduction of hematite nanoparticles by the dissimilatory iron reducing bacterium Shewanella oneidensis MR-1, Geochem. Cosmochim. Acta 73 (4) (2009) 962–976.
[123] A. Fomenko, A. Kondranova, S. Kazantsev, A. Lozkomoev, A. Pervikov, Antimicrobial activity of CuFe2O4 nanoparticles obtained by electric explosion of Fe and Cu wires, in: AIP Conference Proceedings, AIP Publishing LLC, 2019.
[124] E. Glazkova, O. Bakina, N. Rodkevich, A. Mosunov, E. Vornakova, V. Chzhou, M. Lerner, Copper ferrite/copper oxides (I, II) nanoparticles synthesized by electric explosion of wires for high performance photocatalytic and antibacterial applications, Mater. Sci. Eng., B 283 (2022), 115845.
[125] J.P. Novoselova, A.P. Safronov, O.M. Samatov, I.V. Beketov, H. Khurshid, Z. Nemati, H. Srikanth, T.P. Denisova, R. Andrade, G.V. Kurlyandskaya, Laser target evaporation Fe 2 O 3 Nanoparticles for water-based ferrofluids for biomedical applications, IEEE Trans. Magn. 50 (11) (2014) 1–4.
[126] N.G. Semaltianos, G. Karczewski, Laser synthesis of magnetic nanoparticles in liquids and application in the fabrication of polymer–nanoparticle composites, ACS Appl. Nano Mater. 4 (7) (2021) 6407–6440.
[127] A. Safronov, I. Beketov, S. Komogortsev, G. Kurlyandskaya, A. Medvedev, D. Leiman, A. Larrañaga, S. Bhagat, Spherical magnetic nanoparticles fabricated by laser target evaporation, AIP Adv. 3 (5) (2013), 052135.
[128] J.L. Guo, Y.D. Chiou, W.I. Liang, H.J. Liu, Y.J. Chen, W.C. Kuo, C.Y. Tsai, K.A. Tsai, H.H. Kuo, W.F. Hsieh, Complex oxide–noble metal conjugated nanoparticles, Adv. Mater. 25 (14) (2013) 2040–2044.

[129] H. Qin, Y. He, P. Xu, D. Huang, Z. Wang, H. Wang, Z. Wang, Y. Zhao, Q. Tian, C. Wang, Spinel ferrites (MFe2O4): synthesis, improvement and catalytic application in environment and energy field, Adv. Colloid Interface Sci. 294 (2021), 102486.
[130] B. Hussain, Synthesis, Characterization and Antibacterial Study of Silver Doped Manganese Ferrite Nanocomposites, 2021.
[131] H. Du, O.U. Akakuru, C. Yao, F. Yang, A. Wu, Transition metal ion-doped ferrites nanoparticles for bioimaging and cancer therapy, Translational oncology 15 (1) (2022), 101264.
[132] T. Tatarchuk, M. Bououdina, W. Macyk, O. Shyichuk, N. Paliychuk, I. Yaremiy, B. Al-Najar, M. Pacia, Structural, optical, and magnetic properties of Zn-doped CoFe 2 O 4 nanoparticles, Nanoscale Res. Lett. 12 (1) (2017) 1–11.
[133] D.D. Andhare, S.R. Patade, J.S. Kounsalye, K. Jadhav, Effect of Zn doping on structural, magnetic and optical properties of cobalt ferrite nanoparticles synthesized via. Co-precipitation method, Phys. B Condens. Matter 583 (2020), 412051.
[134] M.A. Maksoud, A. El-Ghandour, G.S. El-Sayyad, R.A. Fahim, A.H. El-Hanbaly, M. Bekhit, E. Abdel-Khalek, H. El-Bahnasawy, M. Abd Elkodous, A. Ashour, Unveiling the effect of Zn 2+ substitution in enrichment of structural, magnetic, and dielectric properties of cobalt ferrite, J. Inorg. Organomet. Polym. Mater. 30 (9) (2020) 3709–3721.
[135] M. Atif, M. Asghar, M. Nadeem, W. Khalid, Z. Ali, S. Badshah, Synthesis and investigation of structural, magnetic and dielectric properties of zinc substituted cobalt ferrites, J. Phys. Chem. Solid. 123 (2018) 36–42.
[136] S. Waghmare, D. Borikar, K. Rewatkar, Impact of Al doping on structural and magnetic properties of Co-ferrite, Mater. Today: Proc. 4 (11) (2017) 11866–11872.
[137] R. Dou, H. Cheng, J. Ma, S. Komarneni, Manganese doped magnetic cobalt ferrite nanoparticles for dye degradation via a novel heterogeneous chemical catalysis, Mater. Chem. Phys. 240 (2020), 122181.
[138] J. Lin, Y. He, X. Du, Q. Lin, H. Yang, H. Shen, Structural and magnetic studies of Cr3+ substituted nickel ferrite nanomaterials prepared by sol-gel auto-combustion, Crystals 8 (10) (2018) 384.
[139] M. Abushad, M. Arshad, S. Naseem, H. Ahmed, A. Ansari, V.K. Chakradhary, S. Husain, W. Khan, Synthesis and role of structural disorder on the optical, magnetic and dielectric properties of Zn doped NiFe2O4 nanoferrites, J. Mol. Struct. 1253 (2022), 132205.
[140] A. Nigam, S. Saini, B. Singh, A.K. Rai, S. Pawar, Zinc doped magnesium ferrite nanoparticles for evaluation of biological properties viz antimicrobial, biocompatibility, and in vitro cytotoxicity, Mater. Today Commun. 31 (2022), 103632.
[141] O.K. Mmelesi, R. Patala, T.T. Nkambule, B.B. Mamba, K.K. Kefeni, A.T. Kuvarega, Effect of Zn doping on physico-chemical properties of cobalt ferrite for the photodegradation of amoxicillin and deactivation of E. coli, Colloids Surf. A Physicochem. Eng. Asp. 649 (2022), 129462.
[142] M. Nyathani, G. Sriramulu, T.A. Babu, N. Prasad, D. Ravinder, S. Katlakunta, Crystal chemistry, magnetic and dielectric properties of nickel doped strontium ferrites, Biointerface Res. Appl. Chem. 12 (1) (2021) 929–939.
[143] M.M. Naik, H. Naik, G. Nagaraju, M. Vinuth, K. Vinu, S. Rashmi, Effect of aluminium doping on structural, optical, photocatalytic and antibacterial activity on nickel ferrite nanoparticles by sol–gel auto-combustion method, J. Mater. Sci. Mater. Electron. 29 (23) (2018) 20395–20414.
[144] L. Shao, A. Sun, Y. Zhang, L. Yu, N. Suo, Z. Zuo, Microstructure, XPS and magnetic analysis of Al-doped nickel–manganese–cobalt ferrite, J. Mater. Sci. Mater. Electron. 32 (15) (2021) 20474–20488.
[145] Y. Sun, J. Zhou, D. Liu, X. Li, H. Liang, Enhanced catalytic performance of Cu-doped MnFe2O4 magnetic ferrites: tetracycline hydrochloride attacked by superoxide radicals efficiently in a strong alkaline environment, Chemosphere 297 (2022), 134154.
[146] M.P. Ghosh, S. Mukherjee, Microstructural, magnetic, and hyperfine characterizations of Cu-doped cobalt ferrite nanoparticles, J. Am. Ceram. Soc. 102 (12) (2019) 7509–7520.
[147] R. Jabbar, S.H. Sabeeh, A.M. Hameed, Structural, dielectric and magnetic properties of Mn+ 2 doped cobalt ferrite nanoparticles, J. Magn. Magn Mater. 494 (2020), 165726.
[148] A. Wahab, M. Imran, M. Ikram, M. Naz, M. Aqeel, A. Rafiq, H. Majeed, S. Ali, Dye degradation property of cobalt and manganese doped iron oxide nanoparticles, Appl. Nanosci. 9 (8) (2019) 1823–1832.
[149] N. Lenin, A. Karthik, S. Srither, M. Sridharpanday, S. Surendhiran, M. Balsubramanian, Synthesis, structural and microwave absorption properties of Cr-doped zinc lanthanum nanoferrites Zn1-xCrxLa0. 1Fe1. 9O4 (x= 0.09, 0.18, 0.27 and 0.36), Ceram. Int. (2021).
[150] R. Jasrotia, G. Kumar, K.M. Batoo, S.F. Adil, M. Khan, R. Sharma, A. Kumar, V.P. Singh, Synthesis and characterization of Mg-Ag-Mn nano-ferrites for electromagnet applications, Phys. B Condens. Matter 569 (2019) 1–7.
[151] S.H.U. Din, M.H. Arshed, S. Ullah, P.O. Agboola, I. Shakir, A. Irshad, M. Shahid, Ag-doped nickel ferrites and their composite with rGO: synthesis, characterization, and solar light induced degradation of coloured and colourless effluents, Ceram. Int. 48 (11) (2022) 15629–15639.
[152] D. Jaison, A. Gangwar, P.N. Kishore, G. Chandrasekaran, M. Mothilal, Effect of Gd3+ substitution on proton relaxation and magnetic hyperthermia efficiency of cobalt ferrite nanoparticles, Mater. Res. Express 7 (6) (2020), 064009.
[153] C. Virlan, G. Bulai, O.F. Caltun, R. Hempelmann, A. Pui, Rare earth metals' influence on the heat generating capability of cobalt ferrite nanoparticles, Ceram. Int. 42 (10) (2016) 11958–11965.
[154] K. Zipare, S. Bandgar, G. Shahane, Effect of Dy-substitution on structural and magnetic properties of MnZn ferrite nanoparticles, J. Rare Earths 36 (1) (2018) 86–94.
[155] P. Motavallian, B. Abasht, O. Mirzaee, H. Abdollah-Pour, Correlation between structural and magnetic properties of substituted (Cd, Zr) cobalt ferrite nanoparticles, Chin. J. Phys. 57 (2019) 6–13.
[156] B.D. Kevadiya, A.N. Bade, C. Woldstad, B.J. Edagwa, J.M. McMillan, B.R. Sajja, M.D. Boska, H.E. Gendelman, Development of europium doped core-shell silica cobalt ferrite functionalized nanoparticles for magnetic resonance imaging, Acta Biomater. 49 (2017) 507–520.
[157] A. Zubair, Z. Ahmad, A. Mahmood, W.-C. Cheong, I. Ali, M.A. Khan, A.H. Chughtai, M.N. Ashiq, Structural, morphological and magnetic properties of Eu-doped CoFe2O4 nano-ferrites, Results Phys. 7 (2017) 3203–3208.
[158] W. Mohamed, A.M. Abu-Dief, Impact of rare earth europium (RE-Eu3+) ions substitution on microstructural, optical and magnetic properties of CoFe2−xEuxO4 nanosystems, Ceram. Int. 46 (10) (2020) 16196–16209.
[159] M. Banerjee, A. Mukherjee, A. Banerjee, D. Das, S. Basu, Enhancement of multiferroic properties and unusual magnetic phase transition in Eu doped bismuth ferrite nanoparticles, New J. Chem. 41 (19) (2017) 10985–10991.
[160] J. Cyriac, S. Mathew, S. Augustine, P. Nambissan, Defects characterization studies of europium-substituted bismuth ferrite nanocrystals by positron annihilation and other methods, J. Phys. Appl. Phys. 51 (43) (2018), 435303.
[161] I. Sathisha, K. Manjunatha, V.J. Angadi, B. Chethan, Y. Ravikiran, V.K. Pattar, S. Manjunatha, S. Matteppanavar, Enhanced Humidity Sensing Response in Eu3+-Doped Iron-Rich CuFe Structural, 2O4: A Detailed Study of Microstructural, Sensing, and Dielectric Properties, Mineralogy: Significance and Applications, 2020, p. 75.
[162] S.S. Brahma, J. Nanda, N.K. Sahoo, B. Naik, A.A. Das, Phase transition, electronic transitions and visible light driven enhanced photocatalytic activity of Eu–Ni co-doped bismuth ferrite nanoparticles, J. Phys. Chem. Solid. 153 (2021), 110018.
[163] Z.K. Heiba, M.B. Mohamed, A. El-naggar, A. Albassam, Structure, magnetic and dielectric correlations in indium-doped gallium ferrite, Results Phys. 24 (2021), 104116.
[164] M.P. Ghosh, P. Kumar, M. Kar, S. Mukherjee, Impact of in 3+ ion substitution on microstructural, magnetic and dielectric responses of nickel–cobalt spinel ferrite nanocrystals, J. Mater. Sci. Mater. Electron. 31 (20) (2020) 17762–17772.
[165] R. Jasrotia, V.P. Singh, R. Kumar, M. Singh, Raman spectra of sol-gel auto-combustion synthesized Mg-Ag-Mn and Ba-Nd-Cd-In ferrite based nanomaterials, Ceram. Int. 46 (1) (2020) 618–621.
[166] M. Junaid, M.A. Khan, S.A. Abubshait, M.N. Akhtar, N.A. Kattan, A. Laref, H.M.A. Javed, Structural, spectral, dielectric and magnetic properties of indium substituted copper spinel ferrites synthesized via sol gel technique, Ceram. Int. 46 (17) (2020) 27410–27418.
[167] M. Junaid, M.A. Khan, M.N. Akhtar, A. Hussain, M.F. Warsi, Impact of indium substitution on dielectric and magnetic properties of Cu0. 5Ni0. 5Fe2-xO4 ferrite materials, Ceram. Int. 45 (10) (2019) 13431–13437.

[168] X. Wu, Z. Ding, N. Song, L. Li, W. Wang, Effect of the rare-earth substitution on the structural, magnetic and adsorption properties in cobalt ferrite nanoparticles, Ceram. Int. 42 (3) (2016) 4246–4255.
[169] A. Pachpinde, M. Langade, K. Lohar, S. Patange, S.E. Shirsath, Impact of larger rare earth Pr3+ ions on the physical properties of chemically derived PrxCoFe2− xO4 nanoparticles, Chem. Phys. 429 (2014) 20–26.
[170] M.N. Akhtar, M. Babar, S. Qamar, Z. ur Rehman, M.A. Khan, Structural Rietveld refinement and magnetic features of prosademium (Pr) doped Cu nanocrystalline spinel ferrites, Ceram. Int. 45 (8) (2019) 10187–10195.
[171] S. Kumar, P. Kumar, R. Walia, V. Verma, Improved ferroelectric, magnetic and photovoltaic properties of Pr doped multiferroic bismuth ferrites for photovoltaic application, Results Phys. 14 (2019), 102403.
[172] M.N. Akhtar, M. Yousaf, Y. Lu, M. Baqir, M.A. Khan, M. Ahmad, A. Sarosh, M.S. Nazir, Highly efficient absorber with enhanced magnetoelectric properties based on Y, Gd, and Pr doped NMZ nanoferrites, J. Magn. Magn Mater. 537 (2021), 168232.
[173] S. Keerthana, R. Yuvakkumar, P.S. Kumar, G. Ravi, D. Velauthapillai, Rare earth metal (Sm) doped zinc ferrite (ZnFe2O4) for improved photocatalytic elimination of toxic dye from aquatic system, Environ. Res. 197 (2021), 111047.
[174] S. Singh, P. Kaur, V. Kumar, K. Tikoo, S. Singhal, Traversing the advantageous role of samarium doped spinel nanoferrites for photocatalytic removal of organic pollutants, J. Rare Earths 39 (7) (2021) 781–789.
[175] M. Rhaman, M. Matin, M. Hakim, M. Islam, Bandgap tuning of samarium and cobalt co-doped bismuth ferrite nanoparticles, Mater. Sci. Eng., B 263 (2021), 114842.
[176] M. Rhaman, M. Matin, M. Hossain, M. Khan, M. Hakim, M. Islam, Ferromagnetic, electric, and ferroelectric properties of samarium and cobalt co-doped bismuth ferrite nanoparticles, J. Phys. Chem. Solid. 147 (2020), 109607.
[177] M. Khan, S. Bisen, J. Shukla, A. Mishra, P. Sharma, Investigations on the structural and electrical properties of Sm 3+-doped nickel ferrite–based ceramics, J. Supercond. Nov. Magnetism 34 (3) (2021) 763–780.
[178] M. Abdo, A. El-Daly, Sm-substituted copper-cobalt ferrite nanoparticles: preparation and assessment of structural, magnetic and photocatalytic properties for wastewater treatment applications, J. Alloys Compd. (2021), 160796.
[179] V.J. Angadi, K. Manjunatha, K. Praveena, V.K. Pattar, B.J. Fernandes, S. Manjunatha, J. Husain, S. Angadi, L. Horakeri, K. Ramesh, Magnetic properties of larger ionic radii samarium and gadalonium doped manganese zinc ferrite nanoparticles prepared by solution combustion method, J. Magn. Magn Mater. 529 (2021), 167899.
[180] S.A. Hosseini, Low-cost and eco-friendly viable approach for synthesis of thulium doped copper ferrite nanoparticles using starch, J. Mater. Sci. Mater. Electron. 27 (7) (2016) 7433–7437.
[181] S.A. Hosseini, Novel thulium-doped nickel ferrite: synthesis, characterization, and its photocatalyst application, J. Mater. Sci. Mater. Electron. 27 (11) (2016) 11396–11400.
[182] S. Karimunnesa, A.A. Ullah, M. Hasan, F. Shanta, R. Islam, M. Khan, Effect of holmium substitution on the structural, magnetic and transport properties of CoFe2-xHoxO4 ferrites, J. Magn. Magn Mater. 457 (2018) 57–63.
[183] M.J. Akhter, M.A. Khan, A. Hussain, M.N. Akhtar, M. Ahmad, M.A. Javid, Impact of holmium on structural, dielectric and magnetic properties of Cu–Zn spinel ferrites synthesized via sol–gel route, J. Mater. Sci. Mater. Electron. 32 (2) (2021) 2205–2218.
[184] K. Manjunatha, V.J. Angadi, B.J. Fernandes, K.P. Ramesh, Synthesis and Study of Structural and Dielectric Properties of Dy-Ho Doped Mn-Zn Ferrite Nanoparticles, 2021.
[185] N. Gadwala, D. Ravinder, S. Edapalli, K. Vani, R. Thota, Low Temperature Magnetic Properties of Erbium Doped Bismuth Nano-Ferrites, 2021.
[186] H. Asghara, M. Hussain, S. Aslama, Z. Gilania, M. Ahmedb, M. Khalidd, M. Shifac, M. Afzalc, Tuning the dielectric and structural properties of erbium substitution on cobalt ferrites, Journal of Ovonic Research 17 (4) (2021) 383–394.
[187] G. Vinod, K. Rajashekhar, D. Ravinder, J.L. Naik, Structural, electrical, and magnetic properties of erbium (Er3+) substituted Cu–Cd nano-ferrites, J. Mater. Sci. Mater. Electron. (2021) 1–14.
[188] Z.A. Gilani, A. Farooq, M. Khalid, F.A. Shaikh, S. ul Islam, M.W. Tariq, M.K. Nawaz, S. Yasmeen, Synthesis and Characterization of Lanthanum Doped Co-zn Spinel Ferrites Nanoparticles by Sol-Gel Auto Combustion Method, 2021.
[189] A. Aslam, A.U. Rehman, N. Amin, M.A. un Nabi, Q. ul ain Abdullah, N. Morley, M.I. Arshad, H.T. Ali, M. Yusuf, Z. Latif, Lanthanum doped Zn0. 5Co0. 5LaxFe2− xO4 spinel ferrites synthesized via co-precipitation route to evaluate structural, vibrational, electrical, optical, dielectric, and thermoelectric properties, J. Phys. Chem. Solid. 154 (2021), 110080.
[190] A. Aslam, A. Razzaq, S. Naz, N. Amin, M.I. Arshad, M.A.U. Nabi, A. Nawaz, K. Mahmood, A. Bibi, F. Iqbal, Impact of lanthanum-doping on the physical and electrical properties of cobalt ferrites, J. Supercond. Nov. Magnetism (2021) 1–10.
[191] W. Raza, G. Nabi, A. Shahzad, N. Malik, N. Raza, Electrochemical performance of lanthanum cerium ferrite nanoparticles for supercapacitor applications, J. Mater. Sci. Mater. Electron. 32 (6) (2021) 7443–7454.
[192] T. Roman, D. Ghercă, A.-I. Borhan, M. Grigoraș, G. Stoian, N. Lupu, I. Turcan, N. Cimpoesu, B. Istrate, I. Radu, Nanostructured quaternary Ni1-xCuxFe2-yCeyO4 complex system: cerium content and copper substitution dependence of cation distribution and magnetic-electric properties in spinel ferrites, Ceram. Int. 47 (13) (2021) 18177–18187.
[193] S. Meena, K. Anantharaju, Y. Vidya, L. Renuka, B. Uma, S. Sharma, S.S. More, Enhanced sunlight driven photocatalytic activity and electrochemical sensing properties of Ce-doped MnFe2O4 nano magnetic ferrites, Ceram. Int. 47 (10) (2021) 14760–14774.
[194] K. Hussain, N. Amin, M.I. Arshad, Evaluation of structural, optical, dielectric, electrical, and magnetic properties of Ce3+ doped Cu0. 5Cd0. 25Co0. 25Fe2-xO4 spinel nano-ferrites, Ceram. Int. 47 (3) (2021) 3401–3410.
[195] K.K. Kefeni, T.A. Msagati, B.B. Mamba, Ferrite nanoparticles: synthesis, characterisation and applications in electronic device, Mater. Sci. Eng., B 215 (2017) 37–55.
[196] R. Ranga, A. Kumar, P. Kumari, P. Singh, V. Madaan, K. Kumar, Ferrite application as an electrochemical sensor: a review, Mater. Char. 178 (2021), 111269.
[197] P. Chand, S. Vaish, P. Kumar, Structural, optical and dielectric properties of transition metal (MFe2O4; M= Co, Ni and Zn) nanoferrites, Phys. B Condens. Matter 524 (2017) 53–63.
[198] M. Shakil, U. Inayat, M. Arshad, G. Nabi, N. Khalid, N. Tariq, A. Shah, M. Iqbal, Influence of zinc and cadmium co-doping on optical and magnetic properties of cobalt ferrites, Ceram. Int. 46 (6) (2020) 7767–7773.
[199] M. Margabandhu, S. Sendhilnathan, S. Senthilkumar, D. Gajalakshmi, Investigation of structural, morphological, magnetic properties and biomedical applications of Cu2+ substituted uncoated cobalt ferrite nanoparticles, Braz. Arch. Biol. Technol. 59 (2017).
[200] S. Selima, M. Khairy, M. Mousa, Comparative studies on the impact of synthesis methods on structural, optical, magnetic and catalytic properties of CuFe2O4, Ceram. Int. 45 (5) (2019) 6535–6540.
[201] A.S. Priya, D. Geetha, N. Kavitha, Effect of Al substitution on the structural, electric and impedance behavior of cobalt ferrite, Vacuum 160 (2019) 453–460.
[202] M. Anupama, B. Rudraswamy, N. Dhananjaya, Investigation on impedance response and dielectric relaxation of Ni-Zn ferrites prepared by self-combustion technique, J. Alloys Compd. 706 (2017) 554–561.
[203] N.T. To Loan, N.T. Hien Lan, N.T. Thuy Hang, N. Quang Hai, D.T. Tu Anh, V. Thi Hau, L. Van Tan, T. Van Tran, CoFe2O4 nanomaterials: effect of annealing temperature on characterization, magnetic, photocatalytic, and photo-Fenton properties, Processes 7 (12) (2019) 885.
[204] N. Masunga, O.K. Mmelesi, K.K. Kefeni, B.B. Mamba, Recent advances in copper ferrite nanoparticles and nanocomposites synthesis, magnetic properties and application in water treatment, J. Environ. Chem. Eng. 7 (3) (2019), 103179.
[205] M. Sundararajan, V. Sailaja, L.J. Kennedy, J.J. Vijaya, Photocatalytic degradation of rhodamine B under visible light using nanostructured zinc doped cobalt ferrite: kinetics and mechanism, Ceram. Int. 43 (1) (2017) 540–548.
[206] K.K. Kefeni, B.B. Mamba, T.A. Msagati, Application of spinel ferrite nanoparticles in water and wastewater treatment: a review, Sep. Purif. Technol. 188 (2017) 399–422.

[207] E. Hema, A. Manikandan, M. Gayathri, M. Durka, S.A. Antony, B. Venkatraman, The role of Mn2+-doping on structural, morphological, optical, magnetic and catalytic properties of spinel ZnFe2O4 nanoparticles, J. Nanosci. Nanotechnol. 16 (6) (2016) 5929–5943.
[208] J. Revathi, M.J. Abel, V. Archana, T. Sumithra, R. Thiruneelakandan, Synthesis and characterization of CoFe2O4 and Ni-doped CoFe2O4 nanoparticles by chemical Co-precipitation technique for photo-degradation of organic dyestuffs under direct sunlight, Phys. B Condens. Matter 587 (2020), 412136.
[209] C. Cai, J. Liu, Z. Zhang, Y. Zheng, H. Zhang, Visible light enhanced heterogeneous photo-degradation of Orange II by zinc ferrite (ZnFe2O4) catalyst with the assistance of persulfate, Sep. Purif. Technol. 165 (2016) 42–52.
[210] S. Renukadevi, A.P. Jeyakumari, Rational design of ZnFe2O4/g-C3N4 heterostructures composites for high efficient visible-light photocatalysis for degradation of aqueous organic pollutants, Inorg. Chem. Commun. 118 (2020), 108047.
[211] X. Zhang, B. Lin, X. Li, X. Wang, K. Huang, Z. Chen, MOF-derived magnetically recoverable Z-scheme ZnFe2O4/Fe2O3 perforated nanotube for efficient photocatalytic ciprofloxacin removal, Chem. Eng. J. 430 (2022), 132728.
[212] K. Riaz, S. Nadeem, A. Chrouda, S. Iqbal, A. Mohyuddin, S.U. Hassan, M. Javed, A. BaQais, N. Tamam, K. Aroosh, Coupling of Se-ZnFe2O4 with rGO for spatially charged separated nanocomposites as an efficient photocatalyst for degradation of organic pollutants in natural sunlight, Colloids Surf. A Physicochem. Eng. Asp. 649 (2022), 129332.
[213] Z. Miao, J. Tao, S. Li, J. Wu, Z. Ding, X. Chen, W. Ma, H.-J. Fan, Popcorn-like ZnFe2O4/CdS nanospheres for high-efficient photocatalyst degradation of rhodamine B, Colloids Surf. A Physicochem. Eng. Asp. 654 (2022), 130127.
[214] P. Medeiros, Y.F. Gomes, M. Bomio, I. Santos, M. Silva, C.A. Paskocimas, M. Li, F.V.d. Motta, Influence of variables on the synthesis of CoFe 2 O 4 pigment by the complex polymerization method, Journal of Advanced Ceramics 4 (2) (2015) 135–141.
[215] K. Nechvílová, A. Kalendová, Properties of organic coatings containing pigments with surface modified with a layer of ZnFe2O4. Advances in Science and Technology, Research Journal 9 (28) (2015).
[216] A.J. Ewunkem, L. Rodgers, D. Campbell, C. Staley, K. Subedi, S. Boyd, J.L. Graves, Experimental evolution of magnetite nanoparticle resistance in Escherichia coli, Nanomaterials 11 (3) (2021) 790.
[217] A. Ashour, A.I. El-Batal, M.A. Maksoud, G.S. El-Sayyad, S. Labib, E. Abdeltwab, M. El-Okr, Antimicrobial activity of metal-substituted cobalt ferrite nanoparticles synthesized by sol–gel technique, Particuology 40 (2018) 141–151.
[218] M. Suleman, S. Riaz, In silico study of hyperthermia treatment of liver cancer using core-shell CoFe2O4@ MnFe2O4 magnetic nanoparticles, J. Magn. Magn Mater. 498 (2020), 166143.
[219] T. Dippong, E.A. Levei, O. Cadar, Recent advances in synthesis and applications of MFe2O4 (M= Co, Cu, Mn, Ni, Zn) nanoparticles, Nanomaterials 11 (6) (2021) 1560.